

Received:
9 September 2015
Revised:
1 May 2016
Accepted:
9 May 2016

Heliyon 2 (2016) e00114



Latest Quaternary palaeoceanographic change in the eastern North Atlantic based upon a dinoflagellate cyst event ecostratigraphy

Rex Harland^{a,*}, Irina Polovodova Asteman^b, Audrey Morley^c, Angela Morris^d,
Anthony Harris^d, John A Howe^e

^a 50 Long Acre, Bingham, Nottingham NG13 8AH, UK

^b Uni Research Climate, Bjerknes Centre for Climate Research, Allegaten 55, Bergen NO-5007, Norway

^c School of Geography and Archaeology, National University of Ireland Galway, University Road, Galway, Ireland

^d School of Applied Sciences, University of South Wales, Pontypridd CF37 4AT, UK

^e Scottish Association for Marine Science, Scottish Marine Institute, Oban, Argyll PA37 1QA, UK

* Corresponding author.

E-mail address: rex.harland@ntlworld.com (R. Harland).

Abstract

The analyses of dinoflagellate cyst records, from the latest Quaternary sediments recovered from DSDP Core 610A taken on the Feni Ridge in the southern Rockall Trough, and part of core MD01-2461 on the continental margin of the Porcupine Seabight in the eastern North Atlantic Ocean, has provided evidence for significant oceanographic change encompassing the Last Glacial Maximum (LGM) and part of the Holocene. This together with other published records has led to a regional evaluation of oceanographic change in the eastern North Atlantic over the past 68 ka, based upon a distinctive dinoflagellate event ecostratigraphy. These changes reflect changes in the surface waters of the North Atlantic Current (NAC), and perhaps the deeper thermohaline Atlantic Meridional Overturning Circulation (AMOC), driving fundamental regime changes within the phytoplanktonic communities. Three distinctive dinoflagellate cyst associations based upon both factor and cluster analyses have been recognised. Associations characterised by

Bitectatodinium tepikiense (between 61.1 ± 6.2 to 13.4 ± 1.1 ka BP), *Nematosphaeropsis labyrinthus* (between 10.5 ± 0.3 and 11.45 ± 0.8 ka. BP), and the cyst of *Protoceratium reticulatum* (between 8.5 ± 0.9 and 5.2 ± 1.3 ka. BP) indicate major change within the eastern North Atlantic oceanography. The transitions between these changes occur over a relatively short time span (c.1.5 ka), given our sampling resolution, and have the potential to be incorporated into an event stratigraphy through the latest Quaternary as recommended by the INTIMATE (INTEgrating Ice core, MARine and TERrestrial records) group. The inclusion of a dinoflagellate cyst event stratigraphy would highlight changes within the phytoplankton of the North Atlantic Ocean as a fully glacial world changed to our present interglacial.

Keyword: Earth science

1. Introduction

The surface of the North Atlantic Ocean, between 40 and 50° N, is the most thermally reactive part of the ocean (e.g. Thornalley et al., 2009). This is especially true through the latest part of the Quaternary with sea surface oscillations of >12 °C during glacial/interglacial cycles and the deglaciation record (McIntyre et al., 1976; Lowe and Walker, 1997; Eldevik et al., 2014). This will have considerable effect on the fauna and flora entrained within the surface waters of the ocean. To date, much effort into the dinoflagellate cyst climate signal has concentrated on the neritic realm with less focus on the deep ocean (de Vernal and Marret, 2007). This is explained by less dinoflagellate cyst diversity in the ocean than within the shelf seas (Zonneveld et al., 2013), and until lately by the limited availability of truly oceanic sedimentary sequences for relatively high resolution studies.

This study principally examines the dinoflagellate cyst record from sediments recovered from >2000 m water depth in the eastern Atlantic Ocean, but also includes a comparison with a part record recently completed from the continental margin of the Porcupine Seabight in core MD01-2461 (Peck et al., 2006; Morris, 2011). The provenance of the studied sediments will have both a regional and local signature since they are ultimately derived from a complex regimen of various bottom water currents, the export production from surface water phytoplankton populations, and sources resulting from the dynamics of the British and Irish Ice Sheet (BIIS). In particular, the Norwegian Sea Overflow Current (NSOC) influences both sediment transport and biological content of the contourites of the Feni Ridge (e.g. Jones et al., 1970). Deposition from the nepheloid layer is particularly important in these circumstances and the variability of bottom current activity, as revealed by glaciomarine sediments in both polar oceans and the northeastern Atlantic basin, serves to illustrate the dynamic history of the last

glacial – interglacial cycle with its implications for continuing change (see [Howe et al., 2008](#)).

In addition, the understanding of climate change through the latest Quaternary from both the marine and terrestrial records has long been fraught with difficulties in correlation given certain limitations in precision and accuracy. The INTIMATE (INTEgrating Ice core, Marine and Terrestrial records) group have established a protocol to provide an event stratigraphic approach using the Greenland oxygen isotope record as the stratotype. Although originally focussed on the Last Glacial-Interglacial Transition (LGIT) it now encompasses the last 30–8 ka b2k (before 2000 AD) and includes such climatic events as the Pre-Boreal Oscillation and the 8.2 ka episode ([Hoek et al., 2008](#)), and was most recently expanded to 128 ka b2k ([Blockley et al., 2014](#)). Even so the ordering of events can be difficult because of dating limitations and relevant sampling resolutions ([Lowe et al., 2008](#)). Work on the tephrochronology of the North Atlantic ([Austin et al., 2014](#); [Davies et al., 2014](#)) holds out the promise of increased precision in the establishment of a detailed chronology for the area and hence a better understanding of concomitant environmental change within the marine realm.

The dinoflagellate cyst record described herein from the Feni Ridge and Porcupine Seabight illustrates the potential for including these organisms within an event stratigraphy. This study provides a solid chronostratigraphic dating for the last 34 ka and is quite sufficient to order the dinoflagellate cyst events described herein. To date, and despite the many efforts of various dinoflagellate cyst researchers ([Zumaque et al., 2012](#); [De Schepper, 2013](#); [Bonnet et al., 2013](#); [de Vernal et al., 2013](#); [Rochon et al., 2013](#); [Caulle et al., 2013](#); [Hennissen et al., 2014](#); [Van Nieuwenhove et al., 2016](#)), they remain a ‘Cinderella’ group and are often little utilised in examining the LGIT or even the Quaternary where ultra-high resolution stratigraphic sequences have been recovered from the global ocean. Much recent research concentrates on planktonic foraminifera and the recoverable stable oxygen isotope record (see [Hibbert et al., 2010](#)).

Finally, recent work on the Greenland ice core records reveal marked climatic shifts, of up to 10 °C, during the LGIT occurring on a decadal time scale and sometimes in less than 20 years ([Rasmussen et al., 2006](#); [Rasmussen et al., 2014](#)). Also recent research on the persistence of deep ocean circulation, North Atlantic Deep Water (NADW), during the last interglacial, 128–116 ka, has found that, contrary to it being stable, it was interrupted by several centennial scale reductions in temperature and, at times, accompanied by increased ice rafting and the expansion of polar water ([Galaasen et al., 2014](#)). Our present interglacial, with the prospect of increased ice melting from the Arctic, Greenland and high latitudes, may well mimic this behaviour. Such changes occurring in less than a generation

(Rasmussen et al., 2006; Rasmussen et al., 2014) or over a centennial time scale (Galaasen et al., 2014) are of significant worry in a steadily warming world.

The aim of this study is to provide a dinoflagellate cyst event ecostratigraphy through the LGIT, as the North Atlantic switched from a glacial to interglacial mode. It provides implications for regime change within the surface waters of the Atlantic Ocean and the importance of adding a planktonic proxy to the integrated event stratigraphy. Dinoflagellate cysts are, for instance, a much more diverse group of organisms than the planktonic foraminifera at these latitudes and over this particular time interval (e.g. de Vernal et al., 2000).

2. Materials and methods

Sediment samples have been analysed from both DSDP Hole 610A on the Feni Ridge and from MD01-2461 on the continental margin of the Porcupine Seabight. The first provides data for the main aim of the study whereas the second is included to improve the chronostratigraphy and to emphasise the regional aspect. Both sites are treated separately and described below.

2.1. Hole 610A – Feni Ridge

2.1.1. Introduction

Leg 94 of the Deep Sea Drilling Project (DSDP) was undertaken to investigate bottom-current controlled deposition, known as contourites, from sediment drifts on the Feni Ridge, in the northeastern Atlantic Ocean. These deep sea sediments result from persistent or semi-persistent thermohaline flow and form an archive of ocean circulation that has responded to climate variation (Hollister and Heezen, 1972; De Haas et al., 2003; Rebesco et al., 2014). The Feni Ridge contourite drift is influenced by Arctic Intermediate Water (AIW) originating from the Greenland-Iceland-Norwegian seas and flowing over the Iceland-Scotland Ridge as Norwegian Sea Overflow Water (NSOW) (Robinson and McCave, 1994).

The Feni Ridge is about 600 km in length and up to 700–1000 m thick; it was constructed at the inception of deep-water circulation around the mid-Miocene (~15 Ma) (Jones et al., 1970; Ellett and Roberts, 1973; Laberg et al., 2005). Although the action of the NSOW was probably dominant during preglacial times, Kidd and Hill (1987) suggested its influence decreased as the glacial – interglacial cyclicity became established, and then remained relatively stable over the now relict wave fields.

2.1.2. Study site

Hole 610A was drilled near the axis of the Feni Ridge, at the crest of a sediment wave, on the western side of the Rockall Trough. It was cored in 1983 at Lat: 53°

13.297' N and Long: 18° 53.213' W in 2417 m of water using a hydraulic piston corer (HPC) (Fig. 1). Recovery was excellent at 95% and some 201 m of core was recovered with the oldest sediments being dated as Early Pliocene (NN15). In this study we focus on the deglaciation and Holocene records (Core 1, Sections 1 to 5). Indeed the sediment analysed was assigned to the late Pleistocene – Holocene NN21 and to the diatom *Pseudoeunotia doliolus* Zone (Kidd and Hill, 1987). A full list of the samples studied is provided in Table 1.

2.1.3. Lithology

The sediments recovered in Core 1 are undisturbed interbedded glacial muds to non-glacial nannofossil oozes. However, the photographs of the cores (Ruddiman et al., 1987) suggest some disturbance in the upper part of Core 1, Section 1 as does the somewhat anomalous stable isotope results (see later discussion, Table 1 and Fig. 2. All the studied sediments fall within Unit I of Kidd and Hill (1987), which

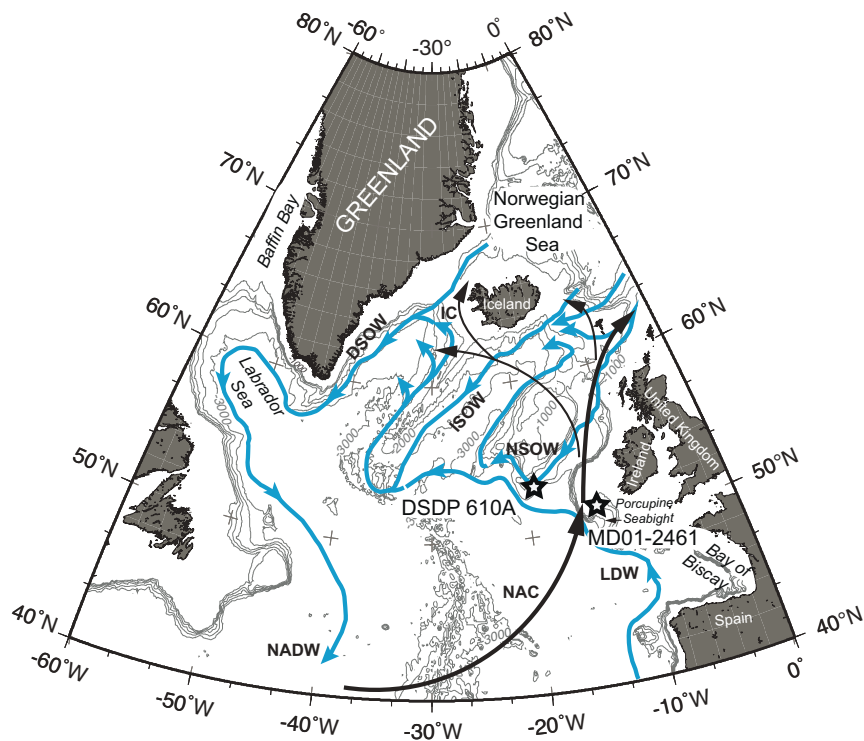


Fig. 1. Map of the northern North Atlantic Ocean showing the sites of DSDP Hole 610A on the Feni Ridge and Core MD01-2461 on the continental margin of the Porcupine Seabight. The blue lines show the course of various deep water flows including the ISOW – Iceland Scotland Overflow Water; the NSOW – Norwegian Sea Overflow Water; the DSOW – Denmark Strait Overflow Water; the NADW – North Atlantic Deep Water and the LDW – Lower Deep Water, following Kissel et al. (2013). The black arrows indicate major surface currents such as the NAC (North Atlantic Current) and the IC (Irminger Current).

Table 1. List of studied samples from DSDP Hole 610A with their British Geological Survey numbers together with their carbon and oxygen stable isotope data.

<u>CSB No.</u>	<u>Hole</u>	<u>Core</u>	<u>Section</u>	<u>Depth (cm)</u>	<u>Cumulative Depth (cm)</u>	<u>$\delta^{13}\text{C}$</u>	<u>$\delta^{18}\text{O}$</u>
10116	610A	1	1	12-14	12-14	-0.26	4.19
10117				30-32	30-32	-0.13	4.1
10118				40-42	40-42	0.03	3.2
10119				60-62	60-62	0.13	3.16
10120				75-77	75-77	0.59	2.97
10121				90-92	90-92	0.49	2.97
10122				106-108	106-108	0.13	2.92
10123				120-122	120-122	0.15	3.16
10124				135-137	135-137	0.3	1.14
10125				148-150	148-150	0.06	1.22
10126		1	2	14-16	164-166	-0.1	3.92
10127				30-32	180-182	-0.13	3.64
10128				38-40	188-190	-0.47	3.84
10129				60-62	210-212	-0.23	3.56
10130				75-79	225-229	-0.27	3.48
10131				88-90	238-240	-0.05	3.57
10132				104-106	254-256	-0.03	3.67
10133				121-123	271-273	-0.02	3.25
10134				134-136	284-286	-0.31	3.82
10135				148-150	298-300	-0.13	3.79
10136		1	3	14-16	314-316	0.14	3.45
10137				30-32	330-332	0.16	3.4
10138				40-42	340-342	-0.05	3.73
10139				60-62	360-362	-0.23	3.81
10140				75-77	375-377	-0.17	3.89
10141				90-92	390-392	-0.03	3.93
10142				106-108	406-408	-0.1	3.72
10143				120-122	420-422	-0.23	3.81
10144				135-137	435-437	-0.43	2.76
10145				148-150	448-450	-0.12	3.24
10146		1	4	12-14	462-464	-0.6	3.17
10147				30-32	480-482	-0.45	3.37
10148				45-47	495-497	-0.48	3.16
10149				60-62	510-512	-0.44	3.16
10150				75-77	525-527	-0.21	2.95

(Continued)

Table 1. (Continued)

<u>CSB No.</u>	<u>Hole</u>	<u>Core</u>	<u>Section</u>	<u>Depth (cm)</u>	<u>Cumulative Depth (cm)</u>	<u>δ13C</u>	<u>δ18O</u>
10151				93-95	543-545	-0.36	3.86
10152				105-107	555-557	-0.38	3.91
10153				120-122	570-572	-0.4	2.96
10154				135-137	585-587	-0.07	3.01
10155				149-151	599-601	-0.03	3.26
10156		1	5	15-17	615-617	0.18	3.02

consists of alternating a) calcareous mud, olive grey to light brown clayey silts with <15% sand; the clay fractions consist of quartz and feldspar with relatively little clay minerals plus volcanic glass and shell fragments together with foraminifera, nannofossil and dropstones and b) white to light grey oozes with <5% terrigenous material and carbonate oozes with 30–60% terrigenous material; foraminifera make up >10%. Contact between the two lithologies is gradational and shows no structures that might relate to current deposition; bioturbation is intense with *Zoophycos*, *Chondrites* and *Planolites* (Kidd and Hill, 1987). In addition dark grey to black volcanic ash occurs as a minor component.

2.1.4. Age model

Sedimentation rates are almost linear and were calculated at between 5 and 6 cm/ka from the Feni and Gaardar drifts (Kidd and Hill, 1987). Interestingly Van Weering and De Rijk (1991) concluded that, at present, a low energy depositional regime exists over the Feni Ridge with an increased influence of the Northeast Atlantic Deep Water (NEADW). Relative dating by the first appearance datum of *Emiliana huxleyi* at Core 2, Section 6, 70–71 cm, equivalent to a drilled depth of 17.3 m (Takayama and Saito, 1987), is generally accepted to occur at 250 ka ago (Shipboard Scientific Party, 2005), and gives a slightly higher sedimentation rate of 6.9 cm/ka. Therefore, the uppermost 616 cm of the core would correspond to about the last 89 ka.

However, our new age model is constrained by five accelerator mass spectrometry (AMS) radiocarbon measurements (¹⁴C) measured at the Keck Carbon Cycle Accelerator Mass Spectrometry facility at UC Irvine, USA. The five samples for radiocarbon dating consist of the planktonic foraminifera *Orbulina universa* and *Globigerina bulloides*, both species have a habitat preference for the upper water column (0–30m) (Anand et al., 2003; Farmer et al., 2007; Jonkers et al., 2013) and are, therefore, well suited to record past surface water ages. Individuals were

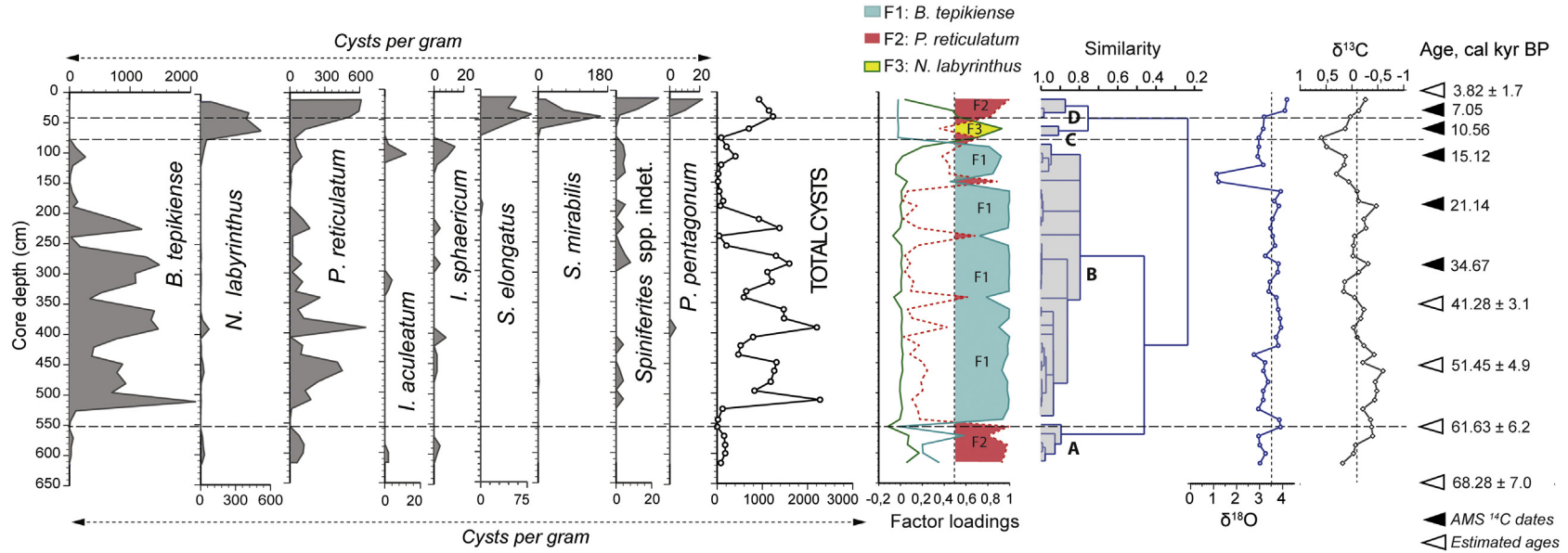


Fig. 2. Dinoflagellate cyst spectrum of selected species from DSDP Hole 610A together with the factor and cluster analyses on the cyst assemblage data and illustrating the three factors and four clusters in relation to the stable oxygen and carbon records taken on planktonic foraminifera. The ages follow the age model based on five AMS ¹⁴C dates (black triangles, for errors, see Table 2) and the Bayesian age-depth modelling extrapolated ages (white triangles). Full data sets are available from the authors on request.

picked at 28, 62, 107, 182 and 284 cm respectively (Table 2). All radiocarbon dates were converted to calendar years with the Calib 7.0.7. software and the MARINE 09 calibration dataset (Stuiver and Reimer, 1993; Stuiver et al., 1998). We applied the implicit reservoir age correction ($\Delta R = 0$) for all dates because the precise reservoir correction for the area is uncertain. In Table 2 we report the weighted mean averages (WMA) of the calibrated probability distribution for each age with their respective 2σ confidence range. The resultant sedimentation rates for the core section between 28 and 284 cm are relatively constant at 9.36 ± 1.6 cm per thousand years, indicating that sedimentation rates over the glacial to interglacial transition did not change greatly (Fig. 3). At an average sampling resolution of 20 cm our record provides a sample approximately every 2000 years. Error estimates for each sample at 95% confidence intervals were calculated using Bacon 2.2, Bayesian age-depth modelling software with the following prior values to begin the Markov-chain Monte Carlo iterations (accumulation shape = 1.5, accumulation mean = 100 years/cm, memory strength = 4, memory mean = 0.7). Largest errors result for samples that fall outside of the dated depths and had to be estimated through extrapolation. At 616 cm the model estimates an age of 68.28 ± 7.0 ka BP. Applying the same approach we obtain an age of 3.82 ± 1.7 ka BP at 0 cm indicating that modern sediments are missing, which is not unusual as these are frequently lost during core recovery.

2.1.5. Processing and statistical techniques

The forty-one samples, taken at approximately 20 cm intervals, were given a standard palynological processing technique involving acid digestion. Basic palynological techniques are described by Wood et al. (1996); also employed was the filtration procedure of Neves and Dale (1963), using Fisons sintered glass funnels of porosity grade 2 (40–90 μm), and the swirling technique of Funkhouser and Evitt (1959) in order to concentrate the dinoflagellate cyst residues. Oxidation was avoided to prevent the possible selective loss of peridiniacean cysts (Dale, 1976; Zonneveld et al., 2008). The use of ultrasound was not required as little amorphous organic material (AOM) was encountered. The resulting palynological residues were stained with Safranin, dispersed onto cover slips and bonded to microscope slides using Petrapoxy 154 resin with a refractive index of 1.54.

The samples were treated quantitatively to calculate the numbers of dinoflagellate cyst species per gram of dry sediment. The original dry weight of sample was noted and aliquot subsamples were taken for mounting and counting (Harland, 1989). Samples were counted from a single slide representing either 1 g of sediment or a fraction thereof using an x 40 objective of a Zeiss Axiolab microscope following earlier work published in Harland (1994). The counts varied from < 10 to > 600 dinoflagellate cysts; the numbers of cysts per gram of sediment, resulting from the recounted and re-examined material, were used to construct a dinoflagellate cyst

Table 2. AMS ^{14}C radiocarbon dates for DSDP Hole 610A.

UCIAMS ID	Exp	Site	Hole	Core	Sect.	Half	top (cm)	bottom (cm)	Planktonic foraminifera	Radiocarbon age	Calibrated age WMA	2 σ range
										$\pm 1\sigma$ error (yr BP)	(cal. ka BP)	(cal. ka BP)
166207	94	610	A	1	1	W	28	30	<i>O. universa</i>	6535 \pm 25	7053	6962 – 7145
166208	94	610	A	1	1	W	62	64	<i>G. bulloides</i>	9660 \pm 25	10556	10476 – 10649
166209	94	610	A	1	1	W	107	109	<i>G. bulloides</i>	13100 \pm 35	15120	14941 – 15277
166210	94	610	A	1	2	W	32	34	<i>G. bulloides</i>	17910 \pm 60	21144	20906 – 21382
166211	94	610	A	1	2	W	134	136.5	<i>G. bulloides</i>	31150 \pm 260	34666	34143 – 35167

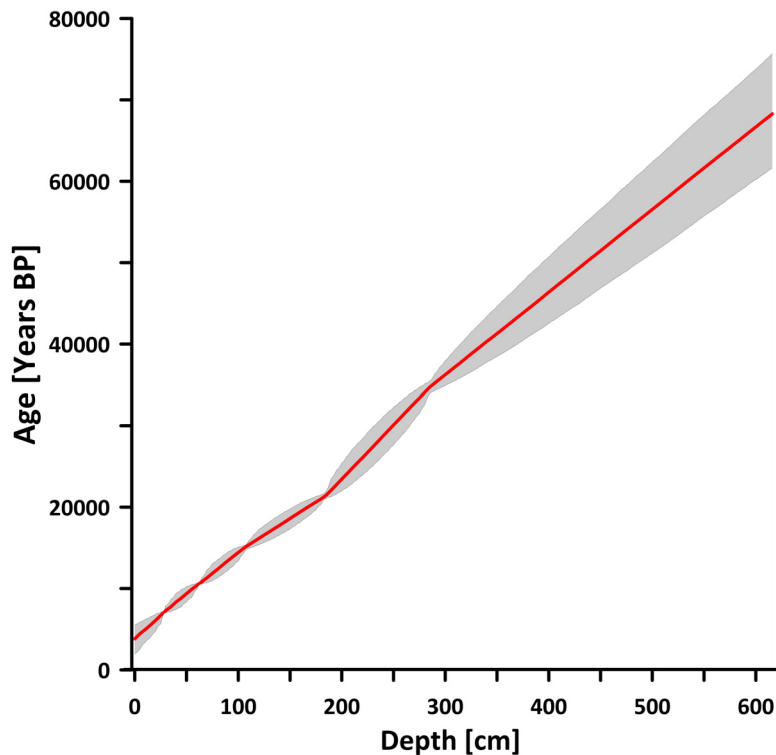


Fig. 3. Age model for the late Quaternary sediments recovered in DSDP Hole 610A based upon 5 AMS 14C dates (Table 2). Error estimates (at 95% confidence intervals) for each sample were calculated using Bacon 2.2 Bayesian age-depth modelling software (see text for details).

spectrum and were also subjected to statistical analyses using the PAST software, University of Oslo (Hammer et al., 2001). The Q-mode cluster analysis was used in preference for this biostratigraphical study in contrast to the R-mode analysis, which is used for clustering of measured variables e.g. associations of various species (Parker and Arnold, 1999). In our study the Q-mode cluster analysis was based on an unweighted pair group average (UPGMA) algorithm and a Pearson's correlation as a similarity index. The UPGMA method creates clusters, which are joined based on the average distance between all members in the two groups. Taking a complement $1-r$ of Pearson's r correlation across the variables makes it a distance measure (Hammer et al., 2001). The UPGMA method was chosen because its dendrograms are known to show the highest cophenetic correlation (Sokal, 1986). Cophenetic correlation approaching 1.0 is a necessary criterion for optimality of the chosen clustering method (Davis, 1986). In our study the UPGMA algorithm and similarity based on Pearson's correlation together yielded a highest cophenetic correlation of 0.85. In order to confirm the presence of observed cluster units we use a parallel multivariate technique i.e. factor analysis as recommended by Parker and Arnold (1999). A simple CABFAC (Calgary and Brown Factor Analysis: Klován and Imbrie, 1971) Q-mode factor analysis with

varimax rotation was performed on data of the most abundant dinoflagellate cysts. The varimax rotation is commonly used to maximize the variance in factor loadings i.e. to increase the explanatory value of factors (Parker and Arnold, 1999).

All the initial counts, the percentage occurrences and the calculated cysts per gram of sediment data together with the prepared slides are held within the archive records of the British Geological Survey, Keyworth, Nottingham, NG12 5GG, UK, (www.bgs.ac.uk).

2.2. Porcupine Seabight

2.2.1. Introduction

Seventeen samples, analysed as a part of a larger study of the Last Glacial Maximum recorded from Core MD01-2461, is included here for comparison, and to assess the geographic extent and timing of the dinoflagellate cyst ecostratigraphy. The material was recovered from the north-western flank of the Porcupine Sea Bight (51° 45' N, 12° 55' W) at a water depth of 1153 m. The core was collected by the Marion Dufresne (campaign reference MD123-Geosciences) in 2001 using a calypso coring device. The total length of the extracted core was 20.23 m but only material from the top 6 m was analysed. The sample data are provided in Table 3 whereas the stratigraphy, counts and statistical treatments are detailed in Morris (2011).

2.2.2. Study site

Core MD01-2461 is situated approximately 160 km offshore of western Ireland (Fig. 1) and is located along the south east margin of the Rockall Trough, a bathymetric depression that runs NNE-SSW. The Porcupine Sea Bight extends about 230 km in a north-south direction, and is 100 km wide at most. It is an embayment of the North Atlantic continental margin bounded to the north by the Slyne Ridge, to the south by the Goban Spur, to the west by the Porcupine Bank and to the east by the Irish Shelf (Moore, 1992). Water depths range from 400 m in the north to more than 3000 m in the southwest, where the embayment opens into the Porcupine Abyssal Plain. Core MD01-2461 was recovered from the north-western flank of the Porcupine Sea Bight.

2.2.3. Lithology

The present-day sedimentation in the area is dominated by hemipelagic inputs (Stow and Tabrez, 1998). Sediments become finer towards the greater depths (Rice et al., 1991). The main sediment supply zone is from the shelves (Celtic and Irish seas), while the input from the Porcupine Bank is much smaller (Rice et al., 1991). The 20.23 m MD01-2461 core recovered olive-grey silty-clay sediments with

Table 3. List of samples selected from the dataset compiled from Morris (2011) from Core MD01-2461 taken on the continental margin, Porcupine Seabight together with their calculated ages.

<u>Sample/Slide no.</u>	<u>Depth (cm)</u>	<u>Ages (ka BP)</u>
336	144.5	8795.605161
335	148.5	9087.479226
328	172.5	10838.72361
327	176.5	11130.59768
320	204.5	13086.44565
319	208.5	13334.68447
391	240.5	15539.998
390	244.5	15668.798
352	294.5	17434.66667
351	298.5	17654
313	370.5	19748.51974
312	374.5	19840.43278
366	429.5	21542.5
258	433.5	21684.498
269	521.5	23963.30133
378	525.5	24029.97
279	601.5	25545.66031

frequent drop stones. Visual observations and x-radiographs did not suggest any evidence of core disturbance or turbidite sequences within the interval studied (Peck et al., 2007b). Sedimentation rates range between 12 and 60 cm ka⁻¹ (Peck et al., 2006) and are considered to have reduced during the Holocene (Øvrebo et al., 2006).

The present-day hydrographic circulation is driven by the formation of intermediate level water, the Labrador Sea Water (LSW) and deeper circulation (NADW). Branches of the NADW mix with the overlying LSW and are recirculated over the Porcupine Abyssal Plain (Van Aken, 2000). Northward flow of warmer, saline surface waters to the Norwegian Sea via the North Atlantic Drift (NAD) and Eastern North Atlantic Waters (ENAW) compensates for this southward penetration of the deep water masses (Peck et al., 2007a). It has been noted that pole-ward flow occurs at all depth levels along the eastern slope of the Porcupine Seabight (Rüggeberg et al., 2005; Rüggeberg et al., 2007), though direct through flow of water below an approximate depth of 500 m is prevented by the morphology of the Porcupine Seabight and currents are topographically steered in a cyclonic direction instead (Frank et al., 2004). ENAW overlies and mixes with

Mediterranean Outflow Water (MOW), which currently bathes the site of MD01-2461 (Peck et al., 2007a) and is characterized by a salinity maximum and oxygen minimum at a depth of 1000–1200 m (Frank et al., 2004).

2.2.4. Age model

An age model for Core MD01-2461 was established by Peck et al. (2006, 2007a, b). Ages are based on 15 AMS ^{14}C dates that have been corrected to a marine reservoir effect of 400 years and then calibrated to calendar years before present (BP) using the CALIB Rev 5.0/MARINE04 data set up to 20 ^{14}C ka BP, and Bard et al. (1998) thereafter. Fine tuning of the radiocarbon age model was further achieved through the correlation of a sea-surface temperature record based on the relative percentages of *Neogloboquadrina pachyderma* sinistral within the assemblage to the GISP2 $\delta^{18}\text{O}$ atmospheric temperature record (Peck et al., 2006). Given that this was calculated using a different calibration curve than that used for the DSDP material we recalibrated all the radiocarbon dates from the MD01-2461 core using the CALIB 3 curve and found that the calibrated ages are not significantly different from those provided in Peck et al. (2006), within their respective 2 sigma error envelopes. Since the age model presented by Peck et al. (2006, 2007a,b) was further fine-tuned using tephra and *N. pachyderma* sinistral abundance counts, there is no need to recalibrate the existing age model for MD01-2461.

2.2.5. Processing and statistical techniques

Although some 150 samples were originally studied (Morris, 2011) only 17 are presented here to compare with sample horizons processed from DSDP 610A. Samples of approximately 1 cm³ were taken at intervals of 4 cm from the upper 6 m of Core MD01-2461, then dried, weighed and processed using acid digestion without oxidation. The palynological residues were filtered using 20 micron sieve polyester mesh. Due to the higher amounts of AOM, these samples were gently sonified using an ultrasonic probe and the final material was mounted on microscope slides and set with glycerine jelly. Samples were selected to correspond with equivalent samples from Core DSDP 610A and were subjected to cluster analysis using PAST and the UPGMA method together with cosine similarity measures, which both resulted in a cophenetic correlation of 0.88.

3. Results

The samples taken from the uppermost part of Hole 610A on the Feni Ridge were analysed to examine the latest Pleistocene/Holocene dinoflagellate cyst stratigraphy. The uppermost ten samples had been the subject of a study published previously by Harland (1994). All samples were re-examined and counted for this

research. A full floral list of the recovered dinoflagellate cysts is presented in Appendix I. Interestingly the samples contained little else except dinoflagellate cysts and the occasional gymnospermous pollen, spores, fungal remains together with some Cretaceous and Paleogene reworking.

A dinoflagellate cyst spectrum of selected species is illustrated in Fig. 2, with the major changes in the cyst assemblages indicated by the informal associations. The statistics (cluster and factor analyses) detail the more significant shifts in the dinoflagellate cyst assemblages.

3.1. Cluster analysis: DSDP Hole 610A

The cluster analysis essentially distinguished four associations that are also subjectively identified by eye from the dinoflagellate cyst spectrum and mark major environmental changes within the record.

Association A. This initial unit encompasses the basal five samples and falls between 555 and 617 cm depth from Core 1, Section 4 to Core 1, Section 5. The age model suggests that this unit can be dated between c. 62.1 ± 6.3 and 68.3 ± 7.0 ka. BP. It is largely characterised by poor recovery, <500 cysts per gram of sediment, assemblages with a diversity never exceeding ten species and largely dominated by the cysts of *Protoceratium reticulatum* (Fig. 4, figure panels 2, 3) with *Nematosphaeropsis labyrinthus* (Fig. 4, figure panels 7, 10) and occasional *Impagidinium* species.

Association B. This second unit encompasses the bulk of the dinoflagellate cyst record. It includes samples from 90–545 cm from Core 1, Section 1 to Core 1, Section 4. A date of 61.1 ± 6.2 to 13.4 ± 1.1 ka BP is suggested based upon the age model. It is characterised by good recovery of mostly >1000 cysts per gram of sediment, and assemblages of never more than ten species. The striking feature of Association B is the high numbers of *Bitectatodinium tepikiense* (Fig. 4, figure panel 1) with the cysts of *Protoceratium reticulatum* and occasional *Impagidinium* and *Spiniferites* species. A second prominent feature of the unit is a number of peak occurrences that can be seen in the numbers of *Bitectatodinium tepikiense* and reflected in the total numbers of dinoflagellate cysts; this feature has also been seen by Zumaque et al. (2012) off the Faeroes. This suggests regular pulses of recruitment to the site of deposition and may have some importance in the final interpretation of the environment of deposition. In particular the dinoflagellate cyst spectrum (Fig. 2) reveals that the youngest part of this unit is characterised by particularly low cyst numbers and is dated at between 21.9 ± 0.8 and 13.4 ± 1.1 ka. BP.

Association C. This unit comprises only two samples taken between 60 and 77 cm depth from Core 1, Section 1. A date of 12.1 ± 1.0 to 10.4 ± 0.4 ka BP is given

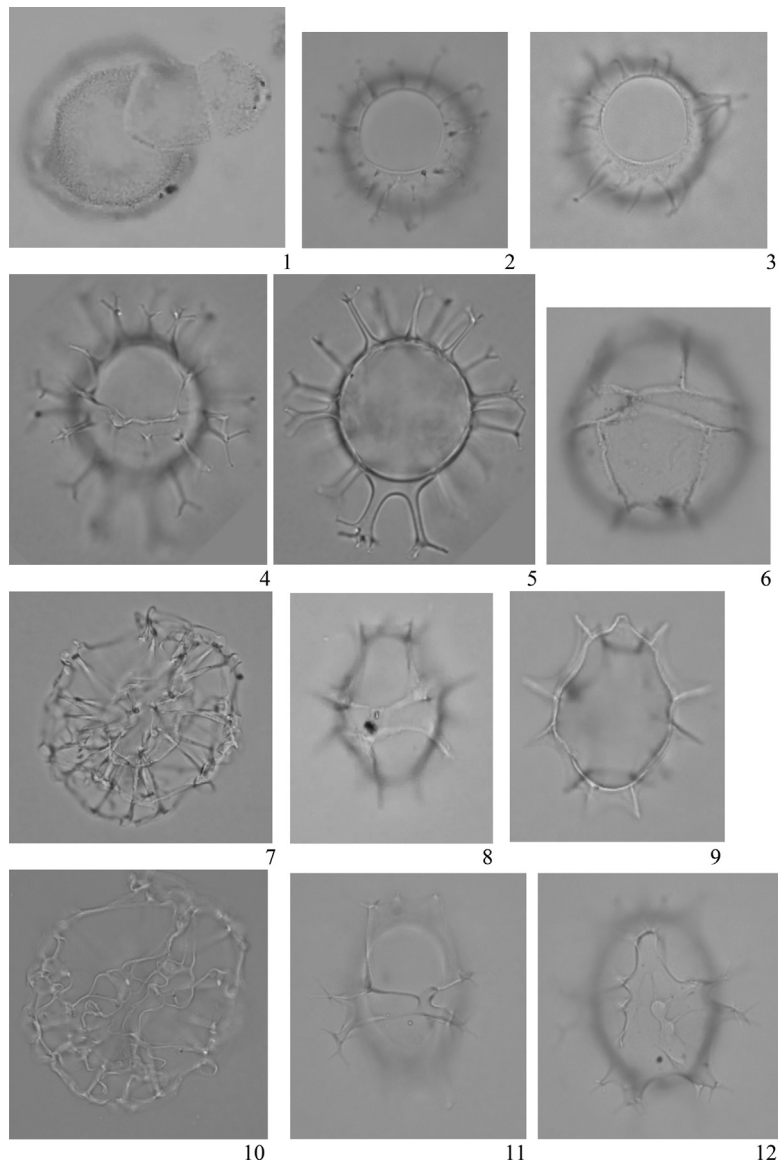


Fig. 4. Panel 1: *Bitectatodinium tepikiense*, MPK 14 553, high focus showing the camarate 3'' and planate 4'' opercula, specimen is 48 μm in diameter, sample CSB 10 129 RH2, England Finder G61/3. Panel 2: Cyst of *Protoceratium reticulatum*, MPK 14 554, low focus showing enlarged 3'' precingular archeopyle, central body is 30 μm in diameter, sample CSB 10 145 RH3, England Finder N38/3. Panel 3: Cyst of *Protoceratium reticulatum*, MPK 14 555, low focus showing the enlarged precingular 3'' archeopyle, central body is 31 μm in diameter, sample CSB 10 116 RH1, England Finder K68/0. Panels 4, 5: *Spiniferites mirabilis*, MPK 14 556, 4. Low focus showing the 3'' precingular archeopyle and the gonal and sutural processes, central body is 47.5 μm in length, sample CSB 10 117 RH1, England Finder J58/0; 5. Median focus showing the nature of the two prominent antapical processes. Panel 6: *Impagidinium sphaericum*, MPK 14 557, low focus showing the 3'' precingular archeopyle and the dorsal paratabulation, central body is 42 μm in length, sample CSB 10 122 RH1, England Finder T55/0. Panels 7, 10: *Nematosphaeropsis labyrinthus*, MPK 14 558, 7. Low focus showing the processes and trabeculae, central body is 62.5 μm in diameter including the processes, sample CSB 10 118 RH1, England Finder Q47/0; 10. High focus showing the trabeculae and position of the archeopyle. Panels 8, 9: *Impagidinium aculeatum*, MPK 14 559, 8. Low focus showing the 3'' precingular archeopyle and nature of the gonal processes, specimen is 32.5 μm in length, sample CSB 10 156 RH1, England Finder S49/4; 9. Median focus showing the intergonal parasutural membranes and the distinctive apical boss. Panels 11, 12: *Spiniferites elongatus*, *Spiniferites* cf. *elongatus* sensu, MPK 14 560. 11. High focus showing the nature of the 3'' precingular archeopyle and the gonal processes, central body is 42.5 μm excluding the processes, sample CSB 10 118, England Finder H60/1; 12. Low focus showing the elongate nature of the central body and the ventral paratabulation by transparency.

based upon the AMS ^{14}C age model. The unit is largely made up of significant numbers of *Nematosphaeropsis labyrinthus* with the cysts of *Protoceratium reticulatum* and occasional *Impagidinium* and *Spiniferites* species. The high numbers of *Nematosphaeropsis labyrinthus* is especially noteworthy and is in contrast to the younger Association D, and to the Porcupine Seabight further east.

Association D. The uppermost unit consists of the final three samples from 12–42 cm depth from Core 1, Section 1. This interval dates between 8.5 ± 0.9 and 5.2 ± 1.3 ka BP and therefore falls within the Holocene Thermal Maximum. They are composed of mostly the cysts of *Protoceratium reticulatum* with *Nematosphaeropsis labyrinthus* and considerable numbers of *Spiniferites elongatus* (Fig. 4, figure panels 11, 12) and *Spiniferites mirabilis* (Fig. 4, figure panels 4, 5) together with *Protoperidinium pentagonum*. This assemblage is similar to modern assemblages from the North Atlantic Ocean (see later discussion). Marked similarities exist between both associations C and D with Holocene dinoflagellate cyst records from the South Icelandic Basin (Eynaud et al., 2004) and MIS 6 and 5 together with MIS 2 in the Bay of Biscay (Penaud et al., 2009).

3.2. Factor analysis

The factor analysis resulted in three factors, which together explain 99.3% of the variance (Table 4). Three dinoflagellate species demonstrated absolute factor scores >1 , which usually implies a high species contribution to the factor (Klovan and Imbrie, 1971) as can be seen in the dinoflagellate cyst spectrum (Fig. 2).

The analysis divides the record into three dinoflagellate cyst associations represented by factors 1–3 (Fig. 2). The first assemblage corresponded to Factor 1 (75.2% of variance), was characterised almost in its entirety by *Bitectatodinium tepikiense* and was exactly equivalent to Association B of the cluster analysis. A second assemblage corresponded to Factor 2 (20.6% of variance) and was characterised by the cysts of dinoflagellate *Protoceratium reticulatum*. This factor is clearly linked to both Associations A and D and makes a small contribution within Association B, having some relationship to the low numbers of *Bitectatodinium tepikiense*. Finally the third assemblage corresponds to Factor 3 (3.6% of variance) and consists almost entirely of *Nematosphaeropsis labyrinthus*; this final assemblage is linked to Association C of the cluster analysis.

Both the cluster analysis and factor analysis identify the same units within the dinoflagellate cyst temporal record. This provides a consistent and potentially significant set of environmental changes within the dinoflagellate populations through the latest Pleistocene and into the Holocene.

The small set of seventeen samples selected from the continental margin of the Porcupine Seabight sediments have been chosen for comparison to the Feni Ridge

Table 4. Varimax scores of dinoflagellate cyst factors defined by CABFAC factor analysis. The bold numbers indicate dinoflagellate species with high (> 1) absolute value of factor scores. The Table also shows eigenvalues and % of variance explained by each factor.

Species	Factor 1	Factor 2	Factor 3
<i>Bitectatodinium tepikiense</i>	4.122	0.030	0.071
<i>Impagidinium aculeatum</i>	0.004	0.029	-0.009
<i>I. pallidum</i>	-0.006	0.041	-0.013
<i>I. paradoxum</i>	5.02E-06	-0.001	0.011
<i>I. patulum</i>	0.004	-0.002	0.002
<i>I. sphaericum</i>	0.018	0.036	0.021
<i>I. striatum</i>	0.0002	-0.001	0.008
<i>Nematosphaeropsis labyrinthus</i>	-0.071	0.429	4.079
<i>Protoceratium reticulatum</i>	-0.023	4.098	-0.437
<i>Spiniferites elongatus</i>	-0.014	0.061	0.265
<i>S. lazus</i>	-0.002	0.018	-0.013
<i>S. membranaceus</i>	-0.001	0.003	0.013
<i>S. mirabilis</i>	-0.027	0.081	0.301
<i>S. ramosus</i>	0.044	0.008	0.014
<i>Spiniferites</i> spp indet.	0.053	0.071	-0.068
<i>Protoperidinium pentagonum</i>	-0.006	0.024	-0.006
<i>Protoperidinium</i> spp indet. [RB]	0.014	-0.011	0.011
Eigenvalues	30.813	8.430	1.466
Variance (%)	75.15	20.56	3.58

material. The full results from the Porcupine Seabight study are presented in Morris (2011) but for comparative purposes the chosen samples have been subjected to cluster analysis. The samples were chosen to link the age model of Hole 610A with the chronostratigraphy of MD01-2461 (see earlier). The dinoflagellate cyst spectrum, based on selected species, is illustrated in Fig. 5. The figure illustrates both the difference in the two sites with DSDP Hole 610A containing a low diversity cyst assemblage in contrast to that of MD01-2461, where the presence of peridiniacean cysts is notable. In contrast there are similarities in the temporal record of the main species such as *Bitectatodinium tepikiense*, *Nematosphaeropsis labyrinthus* and the cysts of *Protoceratium reticulatum* and to a lesser degree with such species as *Impagidinium aculeatum* (Fig. 4, figure panels 8,9), *Impagidinium paradoxum*, *Impagidinium sphaericum* (Fig. 4, figure panel 6), and *Spiniferites mirabilis*.

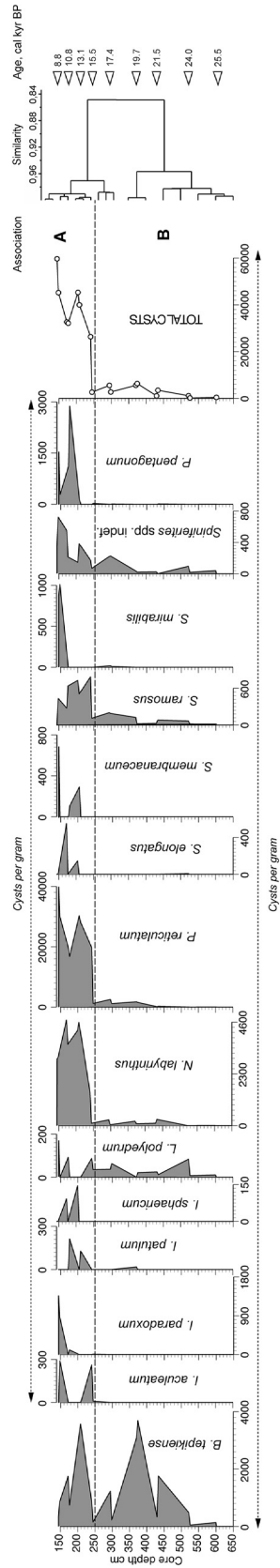


Fig. 5. Dinoflagellate cyst spectrum of selected species from MD01 2461 showing the cluster analysis and the two interpreted associations. Depth in cm. Full data sets are available from the authors on request.

The Porcupine Seabight data only encompasses ages from 8.8 to 25.5 ka BP and, therefore, can only be compared with the upper part of Hole 610A. Nonetheless the assemblage similarities lend weight to the potential of a regional dinoflagellate cyst ecostratigraphic signal. The dinoflagellate cyst spectrum of the samples from the Porcupine Seabight reveal, by visual inspection and cluster analysis, a lower earlier unit B in which dinoflagellate cyst numbers are low, <6000 cysts per gram of sediment, dated between 19.8 and 25.5 ka BP and consisting of predominantly *Bitectatodinium tepikiense* with minor amounts of other species. This was also noted earlier by Zumaque et al. (2012) also recognising *B. tepikiense* as a dominant species within MIS 3. In addition Morris (2011) reported reworked palynomorphs and large amounts of terrestrial phytoclasts linked to land scour by the BIIS. This part of the Porcupine Seabight record is of the same age range as the latest part of Association B recovered from Hole 610A and provides evidence indicating a similar dinoflagellate ecostratigraphy within the LGM in this part of the eastern North Atlantic (see also Zumaque et al., 2012). This older section of the Porcupine Seabight material dominated by *Bitectatodinium tepikiense* also contains significant numbers of *Protoperidinium* spp., the cysts of *Protoceratium reticulatum*, and *Spiniferites* spp. (see also Zumaque et al., 2012). The presence of *Islandinium minutum* (see Morris, 2011) may indicate a subpolar-type environment of colder waters and lower salinities with potentially some sea-ice development (Rochon et al., 1999). Productivity levels may have been low, as indicated by cyst per gram values <7500, with an almost continuous supply of ice-rafted debris to the core site at this time (Peck et al., 2006) coupled with terrestrial phytoclasts from land scour by the adjacent BIIS, indicating further conditions colder than today (Morris, 2011).

Interestingly the younger part of the Porcupine Seabight is characterised by particularly high cyst numbers, >2600 to <60000 consisting of *Bitectatodinium tepikiense*, the cysts of *Protoceratium reticulatum* and *Nematosphaeropsis labyrinthus* (Fig. 5). Morris (2011) noted cyclical changes in dominance between *B. tepikiense* and the cysts of *P. reticulatum* suggesting a periodic strengthening of the North Atlantic Current and some brief returns to cold conditions. This part of the Porcupine Seabight dinoflagellate cyst record, unit B, correlates to the upper part of Associations B on the Feni Ridge. On the continental margin of the Porcupine Seabight a major shift in cyst productivity and a significant of the cysts of *P. reticulatum* takes place at 15.5 ka BP, one of the most significant changes, whereas at Hole 610A the switchover occurs around 10.4 ± 0.4 and 8.5 ± 0.99 ka BP. This suggests a strengthening NAC gradually widening westwards.

Samples from the Porcupine Seabight, equivalent to Cyst Association D from Hole 610A, show significant increases in cyst diversity, notably with *Spiniferites hyperacanthus*, *S. elongatus*, and *S. membranaceus*, and increased numbers of *Impagidinium* species. In addition, these Porcupine Seabight samples from the

earliest Holocene contain a range of *Protoperidinium* species including the cysts of *P. conicum*, *P. leonis*, *P. pentagonum*, and *P. subinermis*, which are not found in Hole 610A, perhaps indicating differences in cyst production across the important ecological boundary between the neritic and oceanic realms along the continental margin together with possible increased water temperatures. The presence of the cyst of *Protoperidinium pentagonum* from around 16.5 ka B.P. also suggests this warming trend, with concentrations peaking at around 11.2 ka B.P. Increased numbers of *Spiniferites mirabilis* appear to follow on from this, and likely indicate that this was the warmest section of the core (Rochon et al., 1999; Penaud et al., 2008). Reduced numbers of terrestrial phytoclasts also represent a period of terrestrially-sourced background sedimentation without glacial scour. Marine productivity was significant at this stage, and an increasing trend is apparent (Morris, 2011).

4. Discussion

The dinoflagellate cyst analysis has revealed a number of clearly distinguishable associations. The first, A, may represent the latest part of an interglacial before the onset of the LGM. However for the moment there is insufficient evidence to comment further except that the occurrence of the cysts of *P. reticulatum* may indicate the activity of the NAC transporting heat to higher latitudes.

A second association, B, with an early part overwhelmingly dominated by *Bitectatodinium tepikiense* (often > 1000 cysts per gram of sediment) and a later part with fewer numbers of the species (often < 100 cysts per gram of sediment) is of particular interest. Zumaque et al. (2012), in their study of MIS 3 south of the Faeroe Shetland Gateway, also found a dominance of *Bitectatodinium tepikiense* suggesting ice free waters and fluctuations matching the evolution of the proximal ice sheets. The cysts of *P. reticulatum* are an important component together with *Spiniferites* spp. and *Impagidinium* forms. The factor analysis picks out a number of horizons where *P. reticulatum* is more represented; this may be indicative of a possible short term change within a fairly monotonous association. The available dating suggests that this association is between 13.4 ± 1.1 and 61.1 ± 6.2 ka BP and an assignment to MIS 2–4. This association certainly correlates with sediments analysed from the Porcupine Seabight and from further south off the coast of Portugal (Zippi, 1992; Turon et al., 2003). The association is consistent with strong seasonality, possible reduction in salinity and cooling of the surface waters. The distribution data for *B. tepikiense* (Zonneveld et al., 2013) show some restriction to sub-polar and temperate seas with SST of -2.0 – 26.9 °C (winter–summer) and SSS of 17.4–39.3 psu (spring–autumn). There is some suggestion that it occurs with sea ice cover of less than four months (de Vernal et al., 1998) whereas Dale (1985) and Bakken and Dale (1986) suggest it may have an association with the polar front. The cyst spectrum reveals a cyst species that has particularly high occurrences on

four occasions within Association B and this may be of some significance. The occurrence of particularly high numbers of *B. tepikiense* (50–95%) between 24.8 ± 2.1 and 57.6 ± 5.7 ka may be indicative of a unique environment as there is no modern analogue in the modern North Atlantic. Interestingly there are no polar species present and the numbers of cysts suggest a well-established thriving dinoflagellate population over a period of some 35 ka or so with occasional warmer components. Cyclical reductions in overall cysts per gram values coincide well with periods around the dates of Heinrich Events H6 to H1 (Hemming, 2004). Towards the later part of the sequence the cyst association is notable for its low numbers, falling to < 500 cysts per gram of sediment. This is dated at between 21.9 ± 0.8 and 13.4 ± 1.1 ka BP and it is surmised that this represents the LGM. In the Porcupine Seabight sequence there is a similar association dated between 25.5 and 15.5 ka BP, thought to be assignable to the LGM. Robinson et al. (1995) show the presence of Heinrich events H3 to H1? over this period within a zone of high IRD. Their reconstruction of the LGM Atlantic Ocean reveals Hole 610A occurring in an area affected by melting icebergs and the warm North East Atlantic Current (NEAC) altogether consistent with the dinoflagellate cyst evidence. Caulle et al. (2013) also document a very similar sequence of events off the south Faeroes. The sporadic occurrences of the cysts of *Protoperidinium reticulatum* may well be associated with Heinrich events and/or pulses of increasing warm water from the NEAC (see also Eynaud et al., 2002).

The younger part of unit B, characterised by low numbers of dinoflagellate cysts (see above) contains a mix of species none of which are particularly dominant. These include *B. tepikiense*, some *Impagidinium* species, *N. labyrinthus*, the cysts of *P. reticulatum* and *Spiniferites* species. This species association is not at all out of place as an extant North Atlantic assemblage. The comparable assemblages from the Porcupine Seabight, also the younger part of unit B, reveal a similar association but perhaps with the addition of the cysts of *Lingulodinium polyedrum* and round, brown *Protoperidinium* cysts. The addition of spores and pollen together with reworked palynomorphs and wood is suggestive of the influence of the BIIS (see Zaragosi et al., 2001; Penaud et al., 2009).

The incoming of the younger association, C, at 12.1 ± 1.0 ka BP marks the most significant change within the dinoflagellate cyst record at DSDP Hole 610A. The sudden disappearance of *B. tepikiense* and the incoming of *N. labyrinthus*, higher numbers of the cysts of *P. reticulatum* and *Spiniferites* species, including both *S. elongatus* and *S. mirabilis*, are noteworthy. It is particularly characterised by the presence of *N. labyrinthus* and by cyst numbers approaching 1000 cysts per gram in the younger of the two samples. At 12.1 ± 1.0 ka BP the earlier part of Association C occurs at the onset of the Pleistocene/Holocene transition at 11.7 calendar yr b2k (Walker et al., 2009). The resolution of the sampling is not, however, sufficient to distinguish the Bølling/Allerød or the Younger Dryas. The

higher resolution Porcupine Seabight samples show increased numbers of the species already mentioned together with *B. tepikiense* (not seen at DSDP 610A), the cyst of *Lingulodinium polyedrum* and the cysts of *Protoperidinium* species (Fig. 5). The species are indicative of an extant North Atlantic assemblage.

Penaud et al. (2009) examined the dinoflagellate cyst record of the LGM to Holocene in the northeastern Atlantic, Southwestern Approaches and the Bay of Biscay, and described high numbers of the cysts of *Protoceratium reticulatum* and an increase in *Nematosphaeropsis labyrinthus* within the Bølling/Allerød. This is similar to the situation described herein but documented in more detail emphasising the use of dinoflagellate cysts in studies of the LGIT.

In the Porcupine Seabight this same association occurs between 11 and 9 ka (Peck et al., 2006) at about the time of the Bølling/Allerød. It is also documented by Eynaud et al. (2004) from the South Icelandic Basin and a little earlier in the Bay of Biscay (Penaud et al., 2009). Zonneveld et al. (2013) regard *N. labyrinthus* as a cosmopolitan species and provide its environmental parameters as SST of -2.1 – 29.8 °C (spring–summer) and SSS of 25.8–39.4 psu (summer–autumn). The occurrence of the species in high numbers has been associated with cooler waters at the beginning of the Holocene before the climatic optimum (Baumann and Matthiessen, 1992). This association has been interpreted as a transition phase before the onset of environments consistent with the modern oceanography but with relatively cool waters before the full effect of the NAC was apparent. This time interval includes the Bølling/Allerød, the Younger Dryas and the early part of the Holocene. Dating from sediments in the Norwegian Sea (Baumann and Matthiessen, 1992) suggests that this association occurs at a later time than herein implying a possible transgressive nature. The suggestion has been made that the occurrence of *N. labyrinthus* is a marker of the passage of the Polar Front over time within the Holocene of the eastern North Atlantic (Caulle et al., 2013). The Younger Dryas is marked in the Porcupine Seabight by a brief increase in *B. tepikiense*.

Finally a fourth association, D, is characterised by the presence of the cysts of *Protoceratium reticulatum*, high cyst numbers (>1000 cysts per gram of sediment), together with significant numbers of *N. labyrinthus*, *Impagidinium* species, *Spiniferites* species and the cyst of *Protoperidinium pentagonum*. The apparent change from high numbers of *N. labyrinthus* in association C to high numbers of the cysts of *P. reticulatum* in association D is noteworthy. This association is dated as 8.5 ± 0.9 ka BP and falls at the beginning of the Holocene Thermal Maximum. Sample resolution is insufficient to provide further detail and there is some suspicion that these younger sediments might be disturbed (see earlier discussion). *P. reticulatum* is known as a cosmopolitan species, which often occurs in high abundance and whose temperature and salinity ranges are SST of -2.1 – 29.8 °C

(spring–summer); SSS of 9.8–39.4 psu (summer) (Zonneveld et al., 2013). It has long been associated with the presence of the North Atlantic Current (NAC). It also occurs as a significant presence within factor F1 with peaks of abundance occur at 462 cm (52.7 ± 5.0 ka BP), 390 cm (45.3 ± 3.9 ka BP) and 340 cm (40.3 ± 2.8 ka BP) respectively (see above).

Earlier work by Zaragosi et al. (2001) had described a threefold warming of the northwestern Bay of Biscay following H2 largely identified by the dinoflagellate cyst associations described above with pulses of NAC penetrations. Add together the studies of Penaud et al. (2009), Eynaud et al. (2012), Zumaque et al. (2012) and Caille et al. (2013) and a much more comprehensive picture of the LGM and LGIT starts to emerge with the analysis of dinoflagellate cysts providing an interesting view of changing sea surface conditions.

The boundary between these four associations appears to be clearly demarked within the dinoflagellate cyst spectra and from both the cluster and factor analysis and coherence with the studies of Zumaque et al. (2012) and Caille et al. (2013). This suggests major environmental shifts during the course of the LGIT, over a wide geographical area, with significant reorganisation of the dinoflagellate populations; a possible regime shift within the phytoplankton?

These dinoflagellate cyst associations can be compared to the distribution maps of the North Atlantic as published by Harland (1983), Turon (1984), Rochon et al. (1999), Marret and Zonneveld (2003) and Zonneveld et al. (2013). Unfortunately the poorly known autecology and the possibility of crypto speciation can detract somewhat from a precise environmental interpretation. The use of statistical techniques such as modern analogue techniques and transfer functions has provided a quantitative approach but the detail is often elusive especially if the provenance of the dinoflagellate cysts is little understood. The analytical approach adopted here is actualistic and reliant upon the known modern distribution data of the species present.

The large increase in cyst per gram values and the significant increases in both cysts of *Protoceratium reticulatum* and *Nematosphaeropsis labyrinthus* in Associations C and D, also seen at an earlier time in the Porcupine Seabight, suggests the establishment of an interglacial regime for the North Atlantic circulation across 53 degrees of latitude at 12.0 ± 1.0 ka BP closely followed by the transition from the early Holocene into the Holocene Thermal Maximum between 10.4 ± 0.4 and 8.5 ± 0.9 ka BP over the Feni Ridge. This is accompanied with a significant rise in SSS, SST_w and a reduction in seasonal temperature contrast, possibly as a result of pulsed freshwater discharge from the European ice sheets and glaciers (Eynaud et al., 2012). The strength of the NAC generally continued to increase, as demonstrated by the appearance of species of *Impagidinium*, *Spiniferites mirabilis*, along with the cysts of *Protoperidinium*

conicum and *Protoperidinium leonis*, possibly also suggesting rising productivity levels, rising SST and/or the influence of a more neritic provenance. For instance Zonneveld et al. (2013) provide the environmental parameters of *S. mirabilis* as SST of -0.8 – 29.8 °C (winter–spring) and SSS of 17.5–39.4 psu (summer–autumn) and regard it as a thermophilic species having a temperate to equatorial distribution.

At the Porcupine Seabight *Nematosphaeropsis labyrinthus* never dominates the cysts of *Protoceratium reticulatum* as it does further west and north. However, in the earliest Holocene, the dominance of *N. labyrinthus* across the Feni Ridge might suggest a phase with a more easterly extension of subpolar waters and hence a narrowing of the path of the NAC. The continued dominance of the cysts *P. reticulatum* along with the appearance of the cysts of *Protoperidinium subinermis* and an increase in *Spiniferites mirabilis* confirms the strong influence of the NAC further east over the Porcupine Seabight.

The preponderance of the three main species requires further comment. The first, the cyst of *Protoceratium reticulatum*, is a cosmopolitan species but in the modern North Atlantic is abundant to dominant, with proportions often $>50\%$. It occurs in more temperate waters where the NAC crosses the Atlantic to Western Europe and flows into the Norwegian and Barents seas elevating both SST and SSS (Fig. 6). This species is, therefore, an effective indicator of this surface current in the eastern North Atlantic (Harland, 1983; Harland, 1988; Zonneveld et al., 2013; Caulle et al., 2013).

The second, *Nematosphaeropsis labyrinthus*, occurs in the highest proportions ($>40\%$) in the western North Atlantic where subpolar waters extend southwards lowering SST and SSS and elevating nutrient levels (Fig. 6 and Fig. 7). In effect it may prove useful in identifying the temporal course of the Polar Front (Caulle et al., 2013). Currently both the cysts of *P. reticulatum* and *N. labyrinthus* form a substantial component of the dinoflagellate cyst assemblages across the North Atlantic.

The third, and perhaps the most important herein, *Bitectatodinium tepikiense* only forms a minor component of modern assemblages and often where SSS are between 30 and 35 psu. However *B. tepikiense* reaches proportions between 10 and 20% in the North Sea and south of Newfoundland close to the Polar Front (Rochon et al., 1999; Zonneveld et al., 2013). These are localities with extreme seasonality, with a February SST more than 3 °C colder than the annual average and more than 5 °C warmer than the annual average in August (Fig. 6 and Fig. 7). This species is not found in regions with extensive ice cover or with SSS reduced by summer meltwater below 30 psu. Interestingly *B. tepikiense* is also found at these proportions in the South Atlantic around the subpolar front offshore Argentina ($\sim 20\%$), an area of extreme seasonality (Zonneveld et al., 2013).

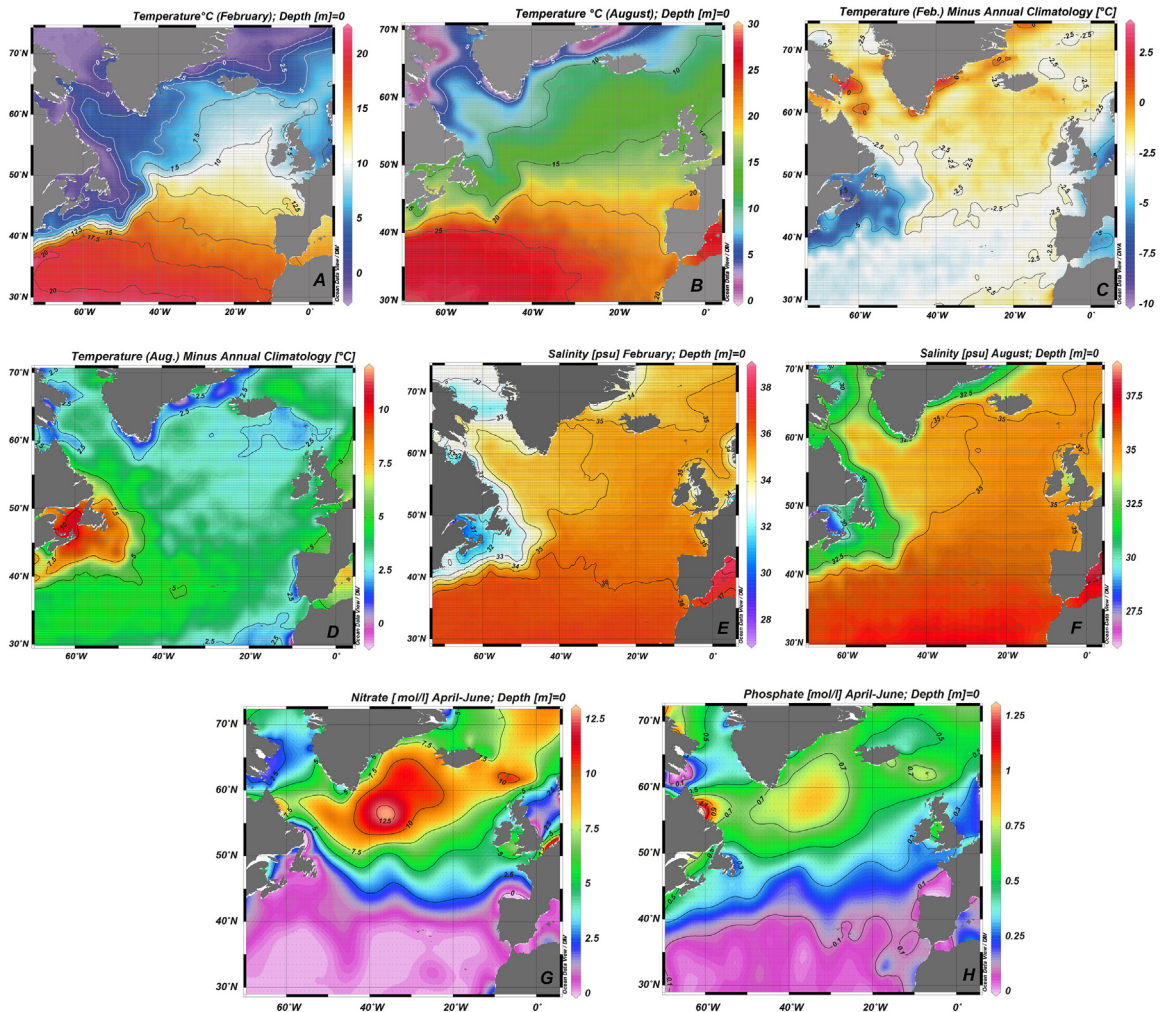


Fig. 6. Objectively analysed mean surface ocean parameters for the North Atlantic: (A) February temperature (°C), (B) August temperature (°C), (C) temperature difference February to annual (°C), (D) temperature difference August to annual (°C), (E) February salinity (psu), (F) August salinity (psu), (G) April to June nitrate concentrations (micro mole/l), (H) April to June phosphate concentrations (micro mole/l). Source Locarnini et al., 2013; Zweng et al., 2013, Garcia et al., 2014a; Garcia et al., 2014b.

The dominance of *B. tepikiense* through the last glacial has no good modern analogue (see above) (de Vernal et al., 2005a). Its dominance here is as a cold water or cryophilic indicator although modern SST tolerances are broad (Zonneveld et al., 2013). Modern occurrences and affinities thus suggest that during much of previous glacial periods in the North Atlantic, the ocean surface over the Feni Ridge and Porcupine Seabight, and extensively from offshore south west Europe and into the Norwegian Sea (Zippi, 1992; Eynaud et al., 2002; de Vernal et al., 2005b), had neither much sea ice nor lowered surface water salinities (SSS >30 psu, Zonneveld et al., 2013). This species was perhaps unique in being able to thrive in waters with extreme seasonality, probably with significantly colder

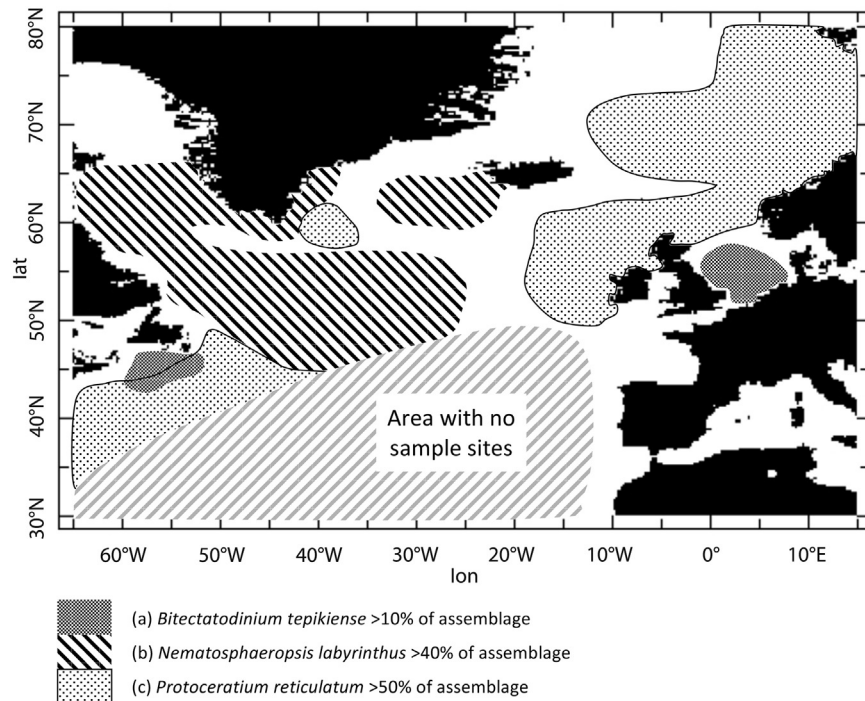


Fig. 7. Distribution of selected dinoflagellate cyst species as a percentage of the assemblages in modern surface sediments from the North Atlantic: (a) *Bitectatodinium tepikiense* >10%, (b) *Nematospaeropsis labyrinthus* >40%, (c) Cyst of *Protoceratium reticulatum* >50%. Area with no sample sites in the 2045 sample database depicted. Adapted from Zonneveld et al. (2013).

winter temperatures but with summer temperatures similar to today (see also Marret et al., 2004 for the Holocene occurrence of *B. tepikiense* in the Celtic Sea). de Vernal et al. (2005b) suggest an affinity for stratified surface waters with a strong seasonal temperature gradient and salinities between 30 and 32 psu. Modern occurrences in areas with low chlorophyll-A (< 2 ml/l; Zonneveld et al., 2013) also suggests that during the glacial period, the extreme seasonality combined with low productivity, provided conditions which other cyst producing dinoflagellate species struggled to tolerate, allowing *B. tepikiense* to flourish without significant competition.

4.1. Comparisons

The use of modern and Quaternary dinoflagellate cysts to elucidate Quaternary stratigraphy has been in use for some time (Harland, 1977). In the late 1980s a dinoflagellate cyst ecostratigraphy began to emerge with the recognition of dinoflagellate cyst associations dominated by *Bitectatodinium tepikiense* giving way to those dominated by *Protoceratium reticulatum* (Harland, 1988). This occurs in the North Sea at the late Pleistocene/Bølling/Allerød boundary at around 13 to 11 ka. BP as ice-dominated waters began to retreat from the North Atlantic.

This dinoflagellate cyst ecostratigraphic event appears to be distinctive, widespread and characteristic (Harland, 1988; Stoker et al., 1989; Duane and Harland, 1990).

In 1992 Zippi published a dinoflagellate cyst analysis of a piston core taken off the continental shelf west of Portugal. This core, TR 174–4, was located at 38° 49' N; 11° 48' W in 4 310 m of water and thought to be close to the position of the Polar Front at around 18 ka. BP. The results indicated a number of consistently occurring species with the downhole incoming of *B. tepikiense* at around the MIS2/1 boundary at 11 ka. BP.

Within Holocene dinoflagellate cyst associations proportional and absolute numbers changed from older assemblages dominated by *N. labyrinthus* to those dominated by the cysts of *P. reticulatum* (Harland 1988). The change from assemblages with high numbers of *B. tepikiense* to those with the cysts of *P. reticulatum* had also been noted by de Vernal et al. (1992) who recognised these as potential ecostratigraphic markers across the Pleistocene/Holocene boundary.

It was becoming apparent that ecostratigraphic correlations within the dinoflagellate cyst associations marked significant oceanographic changes (Turon, 1980; Matthiessen, 1991; de Vernal et al., 1992; Baumann and Matthiessen, 1992). Harland (1994) synthesised the situation for the northeast Atlantic Ocean and noted the peak occurrences of *B. tepikiense*, *N. labyrinthus* and the cysts of *P. reticulatum* as the ocean changed through the LGM to the Holocene. Whereas Harland and Howe (1995) documented cyst associations through the Holocene of the north eastern Atlantic recording the change from an earlier dominated by *N. labyrinthus* to one dominated by the cysts of *P. reticulatum*.

In addition, Rochon et al. (1999) enumerated a series of dinoflagellate cyst assemblages based upon data from 439 sites in the North Atlantic and adjacent seas. In particular they recognised the dominance of *N. labyrinthus* in the Labrador Sea and Irminger Basin and the cysts of *P. reticulatum* in the North Atlantic and Norwegian Sea. Also an assemblage dominated by *B. tepikiense* occurs in a transition zone between the Gulf of St. Lawrence and the North Atlantic Current. Multivariate statistical analyses found that 61.13% of the variance can be explained by SST and SSS (op. cit).

Since that time a number of high resolution studies have been undertaken on sediment sequences contrasting the late Pleistocene/Holocene with the last interglacial. In 2001 Zaragosi et al. (2001) provided a deglaciation record for Bay of Biscay slope environments whereas Eynaud et al. (2004) compared the Holocene and Eemian marine environments within the South Icelandic Basin. Both recognised similar patterns of events to those enumerated here including assemblages with high proportions of *N. labyrinthus* being replaced with assemblages of the cysts of *P. reticulatum*; the former dated between 11.5 to 5.7

ka BP and the latter from 5.7 ka BP to the present. An interpretation of nutrient-rich cool waters giving way to those with higher sea surface temperatures was invoked. In the same year Solignac et al. (2004) looked at Holocene material from the oceanic Iceland Basin and found this same pattern of assemblages indicating cooler waters becoming warmer as the Holocene became established.

Van Nieuwenhove et al. (2013) examined the dinoflagellate cyst floras from both Eemian and Holocene interglacials from the Iceland Plateau. Here again the record from the Iceland Plateau is similar to that recovered from Hole 610A on the Feni Ridge with the distinctive crossover from assemblages with *N. labyrinthus* to those with the cysts of *P. reticulatum*. This was dated at c.6.5 to 8 ka BP such that the North Atlantic was cool temperate with ice present for several months of the year. Thereafter a reduction in the advection of cold waters from the Greenland/East Icelandic Current allowed the incursion of warmer more saline waters into the area with the concomitant loss of sea ice.

In addition Eynaud et al. (2012), Zumaque et al. (2012) and Cauille et al. (2013) have described an increasingly sophisticated picture of changing oceanography through the LGIT linked to glacial pulsed freshwater discharges, ice volumes and the disposition of sea surface currents.

Most recently Van Nieuwenhove et al. (2016) have described changing dinoflagellate cyst associations through the Holocene of the Nordic Seas. Included was the notable changeover between assemblages with *N. labyrinthus* and the cysts of *P. reticulatum* dated between 6.1 and 7.5 ka BP.

A picture of changing oceanography and accompanying phytoplanktonic regime change is beginning to emerge with evidence from the Norwegian Sea (Baumann and Matthiessen, 1992), the Iceland Basin (Eynaud et al., 2004; Solignac et al., 2004), the Nordic seas (Van Nieuwenhove et al., 2016), the Rockall Basin (herein), Bay of Biscay (Zaragosi et al., 2001), the Porcupine Seabight (Duane and Harland, 1990), the eastern North Atlantic off shore Portugal (Zippi, 1992) and the north-eastern Atlantic in general (Cauille et al., 2013). These studies encompass the total eastern North Atlantic between 40° and 70° N over 30° of longitude from off the coast of Portugal to at least 30° W.

5. Conclusions

The dinoflagellate cyst analysis of DSDP Hole 610A has provided a series of dinoflagellate associations spanning a 68 ka possibly from MIS 4 to our present interglacial. These associations have been compared to a new record from off the continental shelf of the Porcupine Seabight and a number of sequences published since the 1980s. It is apparent that these four associations are widespread in the

eastern North Atlantic and point to several re-organisations of the oceanography and the contained phytoplankton populations.

Boundaries separating the various associations are also apparent. These can be enumerated from oldest to youngest:

I – the incoming of large numbers of *Bitectatodinium tepikiense* marking the onset/ establishment of MIS 4 at around 68.3 ± 7.0 ka BP.

II – the incoming of significant numbers of *Nematosphaeropsis labyrinthus* at the beginning of MIS 1. This occurs sometime between 13.4 ± 1.1 and 12.1 ± 1.0 ka BP at the initiation of the Holocene. Due to our low sampling resolution we are unable to differentiate between the Bølling/Allerød, the Younger Dryas and the early Holocene.

III – finally the incoming of cysts of *Protoceratium reticulatum* within MIS 1 as the North Atlantic circulation approaches its present configuration. This occurs between 8.5 ± 0.8 and 10.4 ± 0.4 ka BP over the Feni Ridge and encompasses the Holocene Thermal Maximum.

These boundaries are ecostratigraphic event horizons marking fundamental change within the North Atlantic oceanography. Due to the low sampling resolution and particularly high error estimates for the oldest sections of 610A it is difficult to estimate the exact transition times between associations but there is some evidence to suggest a possible transgressive nature (see [Van Nieuwenhove et al., 2016](#)). Suffice to say that the change from Association A to B appears to take place over a maximum period of 12.5 ka (at the 95% confidence interval) whereas that between Associations B and C and between C and D appear to have taken place over a maximum period of 2 ka and 1.2 ka, respectively. Given the current interest in global change it might be useful to examine these timings rather more carefully as the present ocean becomes increasingly stressed from climate forcing. The use of tephrostratigraphy linked to the Greenland ice-cores as a reference stratotype offers the potential of linking these dinoflagellate cyst associations into a more precise time frame allowing for the assessment of significant regime shifts within the North Atlantic.

This dinoflagellate cyst event stratigraphy is an additional tool to complement the circumscription of the late Pleistocene/Holocene stratigraphy. Dinoflagellate cyst data should be included in any multidisciplinary study aimed at understanding marine environments especially as climate moved from the last glacial to the present day interglacial. This is especially relevant at a time when future impacts on our changing oceans are being considered.

Declarations

Author contribution statement

Rex Harland: Conceived and designed the experiments; Performed the experiments; Analyzed and interpreted the data; Wrote the paper.

Irina Polovodova Asteman, Angela Morris: Performed the experiments; Analyzed and interpreted the data; Contributed reagents, materials, analysis tools or data.

Audrey Morley: Performed the experiments; Analyzed and interpreted the data.

Anthony Harris: Conceived and designed the experiments; Analyzed and interpreted the data; Contributed reagents, materials, analysis tools or data.

John A. Howe: Contributed reagents, materials, analysis tools or data.

Funding statement

This research did not receive any specific grant from funding agencies in the public, commercial, or not-for-profit sectors.

Competing interest statement

The authors declare no conflict of interest.

Additional information

Supplementary content related to this article has been published online at <http://dx.doi.org/10.1016/j.heliyon.2016.e00114>

Acknowledgements

The authors would like to acknowledge the careful palynological processing work undertaken by Ms Jane Kyffin-Hughes at the laboratories of the British Geological Survey (BGS). This study originated as part of Research and Development Programme run in 1990/1991 and entitled 'Dinoflagellate cyst climatostratigraphic synthesis of the Quaternary of the northeastern Atlantic Ocean and British Isles' and followed on from work undertaken as a part of the BGS offshore mapping programme. Special thanks are due to Professor Eystein Jansen at the University of Bergen for his initial support of this research project, the provision of the relevant DSDP samples and for furnishing the stable isotope data. In addition, we thank Professor Charles Wellman, Department of Animal and Plant Sciences, University of Sheffield for the use of their digital photomicrographic facilities. Also we thank Stijn De Schepper, Uni Research Climate and Bjerknes Centre for Climate Research for his most useful discussion on the age model and sharing an office with one of us (IPA). AM and AH would like to thank Ian Hall and Vicky Peck for

access to the MD01-2461 material and their data. We would also like to thank Karin Zonneveld, Martin Head and Jens Matthiessen for their helpful constructive comments on an earlier version of this manuscript and our three reviewers; one of whom, Frédérique Eynaud, was particularly helpful in guiding us to additional relevant literature.

References

- Anand, P., Elderfield, H., Conte, M.H., 2003. Calibration of Mg/Ca thermometry in planktonic foraminifera from a sediment trap time series. *Palaeoceanography* 18, 1–15.
- Austin, W.E.N., Abbot, P.M., Davies, S., Pearce, N.J.G., Wastgard, S., 2014. Marine tephrochronology: an introduction to tracing time in the ocean. In: Austin, W.E.N., Abbot, P.M., Davies, S., Pearce, N.J.G., Wastgard, S. (Eds.), *Marine Tephrochronology*, Special Publication, 398, Geological Society of London, pp. 1–7.
- Bakken, K., Dale, B., 1986. Dinoflagellate cysts in Upper Quaternary sediments from southwestern Norway and potential correlations with the oceanic record. *Boreas* 15, 85–190.
- Bard, E., Arnold, M., Hamelin, B., Tisnerat-Laborde, N., Cabioch, G., 1998. Radiocarbon calibration by means of mass spectrometric $^{230}\text{Th}/^{234}\text{U}$ and ^{14}C ages of corals: An updated database including samples from Barbados, Mururoa and Tahiti. *Radiocarbon* 40, 1085–1092.
- Baumann, K.-H., Matthiessen, J., 1992. Variations in surface water mass conditions in the Norwegian Sea: evidence from Holocene coccolith and dinoflagellate cyst assemblages. *Mar. Micropaleontol.* 20, 129–146.
- Blockley, S.P.E., Bourne, A.J., Brauer, A., Davies, S.M., Hardiman, M., Harding, P.R., Lane, C.S., MacLeod, A., Matthews, I.P., Pyne-O'Donnell, S.D.F., Rasmussen, S.O., Wulf, S., Zanchetta, G., 2014. Tephrochronology and the extended intimate (integration of ice-core, marine and terrestrial records) event stratigraphy 8–128 ka b2k. *Quaternary Sci. Rev.* 106, 88–100.
- Bonnet, S., de Vernal, A., Henry, M., 2013. Dinoflagellate cyst assemblage distributions as tracers of Pacific v. Atlantic water masses in the Northern Hemisphere. In: Lewis, J.M., Marret, F., Bradley, L. (Eds.), *Biological and Geological Perspectives of Dinoflagellates*, 5, The Micropalaeontological Society, Special Publication, Geological Society London, pp. 55–64.
- Caulle, C., Penaud, A., Eynaud, F., Zaragosi, S., Roche, D.M., Michel, E., Boulay, S., Richter, T., 2013. Sea-surface hydrographical conditions off South Faeroes and

within the North-Eastern North Atlantic through MIS 2: the response of dinocysts. *J. Quaternary Sci.* 28, 217–228.

Dale, B., 1976. Cyst formation, sedimentation, and preservation: factors affecting dinoflagellate assemblages in Recent sediments from Trondheimsfjord, Norway. *Rev. Palaeobot. Palyno.* 22, 39–60.

Dale, B., 1985. Dinoflagellate cyst analysis of Upper Quaternary sediments in core GIK15530-4 from the Skagerrak. *Norsk Geol. Tidsskr.* 65, 97–102.

Davies, S.M., Abbott, P.M., Meara, R.H., Pearce, N.J.G., Austin, W.E.N., Chapman, M.R., Svensson, A., Bigler, M., Rasmussen, T.L., Rasmussen, S.O., Farmer, E.J., 2014. A North Atlantic tephrostratigraphical framework for 130-60 ka b2k; new tephra discoveries, marine-based correlations, and future challenges. *Quaternary Sci. Rev.* 106, 101–121.

Davis, J.C., 1986. *Statistics and Data Analysis in Geology*. John Wiley and Sons, New York, pp. 646.

De Haas, H., van Weering, T.C.E., Stoker, M.S., 2003. Development of a sediment drift: Feni Drift, NE Atlantic margin. In: Mienert, J., Weaver, P. (Eds.), *European Marine Sediment Dynamics: side-scan sonar and seismic images*. Springer, Berlin, pp. 107–203.

De Schepper, S., 2013. Combining dinoflagellate cyst studies with geochemical proxies: application to palaeoceanography, palaeoecology and biostratigraphy. In: Lewis, J.M., Marret, F., Bradley, L. (Eds.), *Biological and Geological Perspectives of Dinoflagellates*, 5, The Micropalaeontological Society, Special Publications, Geological Society London, pp. 31–41.

de Vernal, A., Londeix, L., Mudie, P.J., Harland, R., Morzadec-Kerfourn, M.T., Turon, J.-L., Wrenn, J.H., 1992. Quaternary organic-walled dinoflagellate cysts of the North Atlantic Ocean and adjacent seas: ecostratigraphy and biostratigraphy. In: Head, M.J., Wrenn, J.H. (Eds.), *Neogene and Quaternary dinoflagellate cysts and acritarchs*. American Association of Stratigraphic Palynologists Foundation, Dallas, pp. 289–328.

de Vernal, A., Rochon, A., Turon, J.L., Matthiessen, J., 1998. Organic-walled dinoflagellate cysts: palynological tracers of sea-surface conditions in middle to high latitude marine environments. *Geobios* 30, 905–920.

de Vernal, A., Hillaire-Marcel, C., Turon, J.-L., Matthiessen, J., 2000. Reconstruction of sea-surface temperature, salinity, and sea-ice cover in the northern North Atlantic during the last glacial maximum based on dinocyst assemblages. *Can. J. Earth Sci.* 37, 725–750.

de Vernal, A., Hillaire-Marcel, C., Darby, D.A., 2005a. Variability of sea-ice cover in the Chukchi Sea (western Arctic Ocean) during the Holocene. *Paleoceanography*.

de Vernal, A., Eynaud, F., Henry, M., Hillaire-Marcel, C., Londeix, L., Mangin, S., Matthiessen, J., Marret, F., Radi, T., Rochon, A., Solignac, S., Turon, J.-L., 2005b. Reconstruction of sea-surface conditions at middle to high latitudes of the Northern Hemisphere during the Last Glacial Maximum (LGM) based on dinoflagellate cyst assemblages. *Quaternary Sci. Rev.* 24, 897–924.

de Vernal, A., Marret, F., 2007. Organic-walled dinoflagellates: tracers of sea-surface conditions. In: Hillaire-Marcel, C., de Vernal, A. (Eds.), *Proxies in Late Cenozoic Paleoceanography*. Elsevier, The Netherlands, pp. 371–408.

de Vernal, A., Rochon, A., Radi, T., Henry, M., 2013. Dinocysts as proxies for sea-ice cover in Arctic and subarctic environments. In: Lewis, J.M., Marret, F., Bradley, L. (Eds.), *Biological and Geological Perspectives of Dinoflagellates*, 5, The Micropalaeontological Society, Special Publication, Geological Society London, pp. 65–69.

Duane, A., Harland, R., 1990. Late Quaternary dinoflagellate biostratigraphy for sediments of the Porcupine Basin, offshore western Ireland. *Rev. Palaeobot. Palyno.* 63, 1–11.

Eldevik, T., Risebrobakken, B., Bjune, A.E., Andersson, C., Birks, H.J.B., Dokken, T.M., Drange, H., Glessmer, M.S., Li, C., Nilsen, J.E.Ø., Otterå, O.D., Richter, K., Skagseth, Ø., 2014. A brief history of climate –the northern seas from the Last Glacial Maximum to global warming. *Quaternary Sci. Rev.* 106, 225–246.

Ellett, D.J., Roberts, D.G., 1973. The overflow of Norwegian Sea Deep Water across the Wyville-Thomson Ridge. *Deep-Sea Res.* 20, 819–835.

Eynaud, F., Turon, J.L., Duprat, J., 2004. Comparison of the Holocene and Eemian palaeoenvironments in the South Icelandic Basin: dinoflagellate cysts as proxies for the North Atlantic surface circulation. *Rev. Palaeobot. Palyno.* 128, 55–79.

Eynaud, F., Turon, J.L., Matthiessen, J., Kissel, C., Peyrouquet, J.-P., de Vernal, A., Henry, M., 2002. Norwegian Sea surface palaeoenvironments of the Marine Isotopic Stage 3: the paradoxical response of dinoflagellate cysts. *J. Quaternary Sci.* 17, 349–359.

Eynaud, F., Malaizé, B., Zaragosi, S., de Vernal, A., Scourse, J., Pujol, C., Cortijo, E., Grousset, F.E., Penaud, A., Toucanne, S., Turon, J.L., Auffret, G., 2012. New constraints on European glacial freshwater releases to the North Atlantic Ocean. *Geophys. Res. Lett.* 39 L15601.

- Farmer, E.C., Kaplan, A., de Menocal, P.B., Lynch-Stieglitz, J., 2007. Corroborating ecological preferences of planktonic foraminifera in the tropical Atlantic with the stable oxygen isotope ratios of core top specimens. *Paleoceanography* 22, 1–14.
- Frank, N., Paterne, M., Ayliffe, L., van Weering, T., Henriot, J.P., Blamart, D., 2004. Eastern North Atlantic deep-sea corals: tracing upper intermediate water Delta C-14 during the Holocene. *Earth Planet. Sci. Lett.* 219 (3-4), 297–309.
- Funkhouser, J.W., Evitt, W.R., 1959. Preparation techniques for acid-insoluble microfossils. *Micropaleontology* 5, 369–375.
- Galaasen, E.V., Ninnemann, U.S., Irvani, N., Kleiven, H.F., Rosenthal, Y., Kissel, C., Hodell, D.A., 2014. Rapid reductions in North Atlantic Deep Water during the peak of the Last Interglacial. *Science*.
- Garcia, H.E., Locarnini, R.A., Boyer, T.P., Antonov, J.I., Baranova, O.K., Zweng, M.M., Reagan, J.R., Johnson, D.R., 2014a. World Ocean Atlas 2013. Volume 3: Dissolved Oxygen, Apparent Oxygen Utilization, and Oxygen Saturation. In: Levitus, S., Mishonov, A. (Eds.), NOAA Atlas, 75, NESDIS, pp. 27.
- Garcia, H.E., Locarnini, R.A., Boyer, T.P., Antonov, J.I., Baranova, O.K., Zweng, M.M., Reagan, J.R., Johnson, D.R., 2014b. World Ocean Atlas 2013, Volume 4: Dissolved Inorganic Nutrients (phosphate, nitrate, silicate). In: Levitus, S., Mishonov, A. (Eds.), NOAA Atlas, 76, NESDIS, pp. 25.
- Hammer, Ø., Harper, D.A.T., Ryan, P.D., 2001. PAST: Paleontological Statistics Software Package for Education and Data Analysis. *Palaeontol. Electron.* 4, 1–9. Statistical software PAST is available at: <http://folk.uio.no/ohammer/past/>.
- Harland, R., 1977. Recent and Late Quaternary (Flandrian and Devensian) dinoflagellate cysts from the marine continental shelf sediments around the British Isles. *Palaeontographica Abt.B* 164, 87–126.
- Harland, R., 1983. Distribution maps of Recent dinoflagellate cysts in bottom sediments from the North Atlantic Ocean and adjacent seas. *Palaeontology* 26, 311–387.
- Harland, R., 1988. Quaternary dinoflagellate cyst biostratigraphy of the North Sea. *Palaeontology* 31, 78–82.
- Harland, R., 1989. A dinoflagellate cyst record for the last 0.7 Ma from the Rockall Plateau, northeast Atlantic Ocean. *J. Geol. Soc. (London)* 146, 951–954.
- Harland, R., 1994. Dinoflagellate cysts from the Glacial/Postglacial transition in the northeast Atlantic Ocean. *Palaeontology* 37, 263–283.

- Harland, R., Howe, J.A., 1995. Dinoflagellate cysts and Holocene oceanography of the northeastern Atlantic Ocean. *The Holocene* 5, 220–228.
- Hemming, S.R., 2004. Heinrich events: Massive late Pleistocene detritus layers of the North Atlantic and their global climate imprint. *Rev. Geophys.* 42.
- Hennissen, J.A.I., Head, M.J., De Schepper, S., Groeneveld, J., 2014. Palynological evidence for a southward shift of the North Atlantic Current at ~2.6 Ma during the intensification of late Cenozoic Northern Hemisphere glaciation. *Paleoceanography* 28.
- Hibbert, F.D., Austin, W.E.N., Leng, M.J., Gatliff, R.W., 2010. British Ice Sheet dynamics inferred from North Atlantic ice-rafted debris records spanning the last 175 000 years. *J. Quaternary Sci.* 25, 461–482.
- Hoek, W.Z., Yu, Z.C., Lowe, J.J., 2008. INTEgration of Ice-core, Marine, and Terrestrial records (INTIMATE): refining the record of the Last Glacial-Interglacial Transition. *Quaternary Sci. Rev.* 27, 1–5.
- Hollister, C.D., Heezen, B.C., 1972. Geologic effects of ocean bottom currents: western North Atlantic. In: Godron, A.L. (Ed.), *Studies in physical oceanography* 2. Gordon and Breach, New York, pp. 37–66.
- Howe, J.A., Shimmield, T.M., Harland, R., 2008. Late Quaternary contourites and glaciomarine sedimentation in the Fram Strait. *Sedimentology* 55, 179–200.
- Jones, E.J.W., Ewing, M., Ewing, J.I., Etreim, S.L., 1970. Influences of Norwegian Sea Overflow Water on sedimentation in the northern North Atlantic and Labrador Sea. *J. Geophys. Res.* 75, 1655–1680.
- Jonkers, L., van Heuven, S., Zahn, R., Peeters, F.J.C., 2013. Seasonal patterns of shell flux, $\delta^{18}\text{O}$ and $\delta^{13}\text{C}$ of small and large *N. pachyderma* (s) and *G. bulloides* in the subpolar North Atlantic. *Paleoceanography* 28, 164–174.
- Kidd, R.B., Hill, P.R., 1987. Sedimentation on Feni and Gaardar sediment drifts. Initial Reports of the Deep Sea Drilling Project 94, 1217–1244.
- Klovan, J.E., Imbrie, J., 1971. An algorithm and FORTRAN-IV program for large scale Q-mode factor analysis and calculation of factor scores. *Math. Geol.* 3, 61–77.
- Kissel, C., van Toer, A., Laj, C., Cortijo, E., Michel, E., 2013. Variations in the strength of the North Atlantic bottom water during the Holocene. *Earth and Planetary Science Letters* 369-370, 248–259.
- Laberg, J.S., Stoker, M.S., Dahlgren, T.K.I., Haas, H., Hafliðason, H., Hjelstuen, B., Nielsen, T., Shannon, P., Vorren, T., van Weering, T.C.E., Ceramicola, S.,

2005. Cenozoic alongslope processes and sedimentation on the NW European Atlantic margin. *Mar. Petrol. Geol.* 22, 1069–1088.

Locarnini, R.A., Mishonov, A.V., Antonov, J.I., Boyer, T.P., Garcia, H.E., Baranova, O.K., Zweng, M.M., Paver, C.R., Reagan, J.R., Johnson, D.R., Hamilton, M., Seidov, D., 2013. World Ocean Atlas 2013, Volume 1: Temperature. In: Levitus, S., Mishonov, A. (Eds.), NOAA Atlas, 73, NESDIS, pp. 40.

Lowe, J.J., Rasmussen, S.O., Björök, S., Hoek, W.Z., Steffensen, J.P., Walker, M.J.C., Yu, Z.C., the INTIMATE group, 2008. Synchronisation of palaeoenvironmental events in the North Atlantic region during the Last Termination: a revised protocol recommended by the INTIMATE group. *Quaternary Sci. Rev.* 27, 6–17.

Lowe, J.J., Walker, M.J.C., 1997. *Reconstructing Quaternary Environments*. Routledge, London, pp. 472.

Marret, F., Zonneveld, K.A.F., 2003. Atlas of modern organic-walled dinoflagellate cyst distribution. *Rev. Palaeobot. Palyno.* 125, 1–200.

Marret, F., Scourse, J., Austin, W., 2004. Holocene shelf-sea stratification dynamics: a dinoflagellate cyst record from the Celtic Sea, NW European shelf. *The Holocene* 14, 689–696.

Matthiessen, J., 1991. Dinoflagellaten-Zysten im Spätquartär des europäischen Nordmeeres: Palökologie und Paläo-oceanographie. *Geomar Report* 7, 1–104.

McIntyre, A., Kipp, N.G., Bé, A.W.H., Crowley, T., Kellogg, T., Gardner, J.V., Prell, W., Ruddiman, W.F., 1976. Glacial North Atlantic 18,000 years ago: a CLIMAP reconstruction. *Geol. Soc. Am. Mem.* 145, 43–76.

Moore, J.G., 1992. A syn-rift to post-rift transition sequence in the Main Porcupine Basin, offshore western Ireland. In: Parnell, J. (Ed.), *Basins on the Atlantic Seaboard: Petroleum Geology, Sedimentology and Basin Evolution*, 62, Geological Society Special Publications, pp. 333–349.

Morris, A., 2011. Relating ice, ocean and climate interactions in the north east Atlantic from the last glacial maximum to the Holocene using marine palynology. Unpublished Ph.D. Thesis. University of South Wales, 239.

Neves, R., Dale, B., 1963. A modified filtration system for palynological preparation. *Nature* 198, 775–776.

Øvrebø, L.K., Haughton, P.D.W., Shannon, P.M., 2006. A record of fluctuating bottom currents on the slopes west of the Porcupine Bank, offshore Ireland — implications for Late Quaternary climate forcing. *Mar. Geol.* 225, 279–309.

- Parker, W.C., Arnold, A.J., 1999. Quantitative methods of data analysis in foraminiferal ecology. In: Sen Gupta, B.K. (Ed.), *Modern Foraminifera*. Kluwer Academic Publishers, pp. 71–89.
- Peck, V.L., Hall, I.R., Zahn, R., Elderfield, H., Grousset, F., Hemming, S.R., Scourse, J.D., 2006. High resolution evidence for linkages between NW European ice sheet instability and Atlantic meridional overturning circulation. *Earth and Planet. Sci. Lett.* 243, 476–488.
- Peck, V.L., Hall, I.R., Zahn, R., Grousset, F., Hemming, S.R., Scourse, J.D., 2007a. The relationship of Heinrich events and their European precursors over the past 60 ka BP: a multi-proxy ice-rafted debris provenance study in the north east Atlantic. *Quaternary Sci. Rev.* 26, 862–875.
- Peck, V.L., Hall, I.R., Zahn, R., Scourse, J.D., 2007b. Progressive reduction in NE Atlantic intermediate water ventilation prior to Heinrich events: response to NW European ice sheet instabilities? *Geochem. Geophys.* 8.
- Penaud, A., Eynaud, F., Turon, J.L., Zaragosi, S., Marret, F., Bourillet, J.F., 2008. Interglacial variability (MIS 5 and MIS 7) and dinoflagellate cysts assemblages in the Bay of Biscay (North Atlantic). *Mar. Micropaleontol.* 68, 136–155.
- Penaud, A., Eynaud, F., Turon, J.L., Zaragosi, S., Malaize, B., Toucanne, S., Bourillet, J.F., 2009. What forced the collapse of European ice sheets during the last two glacial periods (150 ka B.P. and 18 ka cal B.P.)? Palynological evidence. *Palaeogeogr. Palaeoclimatol.* 281 (1-2), 66–78.
- Rasmussen, S.O., Andersen, K.K., Svensson, A.M., Steffensen, B.M., Vinther, B. M., Clausen, H.B., Siggaard-Andersen, M.-L., Johnsen, S.J., Larsen, L.B., Dahl-Jensen, D., Bigler, M., Röthlisberger, R., Fischer, H., Goto-Azuma, K., Hansson, M.E., Ruth, U., 2006. A new Greenland ice core chronology for the last glacial termination. *J. Geophys. Res.* 111, D06102.
- Rasmussen, S.O., Bigler, M., Blockley, S.P., Blunier, T., Buchardt, S.L., Clausen, H.B., Cvijanovic, I., Dahl-Jensen, D., Johnsen, S.J., Fischer, H., Gkinis, V., Guillevic, M., Hoek, W.Z., Lowe, J.J., Pedro, J.B., Popp, T., Seierstad, I.K., Steffensen, J.P., Svensson, A.M., Vallelonga, P., Vinther, B.M., Walker, M.J.C., Wheatley, J.J., Winstrup, M., 2014. A stratigraphic framework for abrupt climatic changes during the Last Glacial period based on three synchronized ice-core records: refining and extending the INTIMATE event stratigraphy. *Quaternary Sci. Rev.* 106, 14–28.
- Rebesco, M., Hernández-Molina, F.J., Van Rooij, D., Wåhlin, A., 2014. Contourites and associated sediments controlled by deep-water circulation processes: State-of-the-art and future considerations. *Mar. Geol.* 352, 111–154.

- Rice, A.L., Billet, D.S.M., Thurston, M.H., Lampitt, R.S., 1991. The Institute of Oceanographic Sciences biology programme in the Porcupine Sea Bight: background and general introduction. *J. Mar. Biol. Assoc. UK* 71, 281–310.
- Robinson, S.G., Maslin, M.A., McCave, I.N., 1995. Magnetic susceptibility variations in Upper Pleistocene deep-sea sediments of the NE Atlantic: implications for ice rafting and paleocirculation at the last glacial maximum. *Paleoceanography* 10, 221–250.
- Robinson, S.G., McCave, N., 1994. Orbital forcing of bottom-current enhanced sedimentation on Feni Drift, NE Atlantic during the mid-Pleistocene. *Paleoceanography* 9, 943–972.
- Rochon, A., de Vernal, A., Turon, J.-L., Matthiessen, J., Head, M.J., 1999. Distribution of recent dinoflagellate cysts in surface sediments from the North Atlantic Ocean and adjacent seas in relation to sea-surface parameters. *American Association of Stratigraphic Palynologists Contribution Series* 35, 1–146.
- Rochon, A., Harland, R., de Vernal, A., 2013. Dinoflagellates and their cysts: key foci for future research. In: Lewis, J.M., Marret, F., Bradley, L. (Eds.), *Biological and Geological Perspectives of Dinoflagellates*, 5, The Micropalaeontological Society, Special Publication, Geological Society London, pp. 89–95.
- Ruddiman, W.F., Kidd, R.B., Thomas, E., et al., 1987. Site 610. *Initial Reports of the Deep Sea Drilling Project* 94, 351–470.
- Rüggeberg, A., Dorschel, B., Dullo, W., Hebbeln, D., 2005. Sedimentary patterns in the vicinity of a carbonate mound in the Hovland Mound Province, northern Porcupine Seabight. In: Freiwald, A., Roberts, J.M. (Eds.), *Cold-water Corals and Ecosystems*. Springer-Verlag, Berlin, Heidelberg, pp. 87–112.
- Rüggeberg, A., Dullo, W.C., Dorschel, B., Hebbeln, D., 2007. Environmental changes and growth history of a cold-water carbonate mound (Propeller Mound, Porcupine Seabight). *Int. J. Earth Sci.* 96, 57–72.
- Shipboard Scientific Party,, 2005. North Atlantic climate: ice sheet–ocean atmosphere interactions on millennial timescales during the late Neogene–Quaternary using a paleointensity-assisted chronology for the North Atlantic. *IODP Preliminary Report* 303, 1–51 <http://iodp.tamu.edu/publications/PR/303PR/303PR.PDF>.
- Sokal, R.R., 1986. Phenetic taxonomy: Theory and methods. *Annu. Rev. Ecol. Syst.* 17, 423–442.
- Solignac, S., de Vernal, A., Hillaire-Marcel, C., 2004. Holocene sea-surface conditions in the North Atlantic –contrasted trends and regimes in the western and eastern sectors (Labrador Sea vs Iceland Basin). *Quaternary Sci. Rev.* 23, 319–334.

Stoker, M.S., Harland, R., Morton, A.C., Graham, D.K., 1989. Late Quaternary stratigraphy of the northern Rockall Trough and Faroe-Shetland Channel, northeast Atlantic Ocean. *J. Quaternary Sci.* 4, 211–222.

Stow, D.A.V., Tabrez, A.R., 1998. Hemipelagites: processes, facies and models. In: Stoker, M.S., Evans, D., Cramp, A. (Eds.), *Geological Processes on Continental Margins: Sedimentation, Mass-Wasting and Stability*, 129, Geological Society of London Special Publication, pp. 317–337.

Stuiver, M., Reimer, P.J., 1993. Extended ^{14}C data-base and revised calib 3.0 ^{14}C age calibration program. *Radiocarbon* 35, 215–230.

Stuiver, M., Reimer, P.J., Bard, E., Beck, W., Burr, G.S., Hughen, K.A., Kromer, B., McCormac, G., van der Plicht, J., Spurk, M., 1998. INTCAL98 radiocarbon age calibration, 24,000-0 cal BP. *Radiocarbon* 40, 1041–1083.

Takayama, T., Saito, T., 1987. Coccolith biostratigraphy of the North Atlantic Ocean, Deep Sea Drilling Project Leg 94. *Initial Reports of the Deep Sea Drilling Project 94*, 651–702.

Thornalley, D.J.R., Elderfield, H., McCave, I.N., 2009. Holocene oscillations in temperature and salinity of the surface subpolar North Atlantic. *Nature* 457 (5), 711–714.

Turon, J.-L., 1980. Dinoflagellés et environnement climatique. Les kystes de dinoflagellés dans les sédiments Récents de l'Atlantique nord-oriental et leurs relations avec l'environnement océanique. Application aux dépôts Holocènes du Chenal de Rockall. *Mémoires du Muséum Nationale d'Histoire Naturelle B27*, 269–282.

Turon, J.-L., 1984. Le palynoplancton dans l'environnement de l'Atlantique nord-oriental; evolution climatique et hydrologique depuis le dernier maximum glaciaire. *Memoires de l'Institut de Geologie du Bassin d'Aquitaine* 17, 1–313.

Turon, J.-L., Lézine, A.-M., Denèfle, M., 2003. Land-sea correlations for the last glaciation inferred from a pollen and dinocyst record from the Portuguese margin. *Quaternary Res.* 59, 88–96.

Van Aken, H.M., 2000. The hydrology of the mid-latitude Northeast Atlantic Ocean: I, The deep water masses. *Deep-Sea Res. Pt. I* 47, 757–788.

Van Nieuwenhove, N., Bauch, H.A., Andruleit, H., 2013. Multiproxy fossil comparison reveals contrasting surface ocean conditions in the western Iceland Sea for the last two interglacials. *Palaeogeogr. Palaeoclimatol. Palaeoecol.* 370, 247–259.

Van Nieuwenhove, N., Baumann, A., Matthiessen, J., Bonnet, S., de Vernal, A., 2016. Sea surface conditions in the southern Nordic Seas during the Holocene based on dinoflagellate cyst assemblages. *The Holocene*, 1–14.

Van Weering, T.C.E., De Rijk, S., 1991. Sedimentation and climate-induced sediments on Feni Ridge, northeast Atlantic Ocean. *Mar. Geol.* 101, 49–69.

Walker, M., Johnsen, S., Rasmussen, S.O., Popp, T., Steffensen, J.-P., Gibbard, P., Hoek, W., Lowe, J., Andrews, J., Björck, S., Cwynar, L.C., Hughen, K., Kershaw, P., Kromer, B., Litt, T., Lowe, D.J., Nakagawa, T., Newnham, R., Schwander, J., 2009. Formal definition and dating of the GSSP (Global Stratotype Section and Point) for the base of the Holocene using the Greenland NGRIP ice core, and selected auxiliary records. *J. Quaternary Sci.* 24, 3–17.

Wood, G.D., Gabriel, A.M., Lawson, J.C., 1996. Palynological techniques? processing and microscopy. In: Jansonius, J., McGregor, D.C. (Eds.), *Palynology: principles and applications*, 1, American Association of Stratigraphic Palynologists Foundation, Salt Lake City, pp. 29–50.

Zaragosi, S., Eynaud, F., Pujol, C., Auffret, G.A., Turon, J.-L., Garlan, T., 2001. Initiation of the European deglaciation as recorded in the northwestern Bay of Biscay slope environments (Meriadzek Terrace and Trevelyan Escarpment): a multi-proxy approach. *Earth Planet. Sci. Lett.* 188, 493–507.

Zippi, P.A., 1992. Dinoflagellate cyst stratigraphy and climate fluctuations in the eastern North Atlantic during the last 150,000 years. In: Head, M.J., Wrenn, J.H. (Eds.), *Neogene and Quaternary dinoflagellate cysts and acritarchs*. American Association of Stratigraphic Palynologists Foundation, Dallas, pp. 55–68.

Zonneveld, K.A.F., Versteegh, G., Kodrans-Nsiah, M., 2008. Preservation and organic chemistry of Late Cenozoic organic-walled dinoflagellate cysts: A review. *Mar. Micropaleontol.* 68, 179–197.

Zonneveld, K.A.F., Marret, F., Versteegh, G.J.M., Bogus, K., Bonnet, S., Bouimetarhan, I., Crouch, E., de Vernal, A., Elshanawany, R., Edwards, L., Esper, O., Forke, S., Grøsfjeld, K., Henry, M., Holzwarth, U., Kielt, J.-F., Kim, S.-Y., Ladouceur, S., Ledu, D., Chen, L., Limoges, A., Londeix, L., Lu, S.-H., Mahmoud, M.S., Marino, G., Matsouka, K., Matthiessen, J., Mildenhall, D.C., Mudie, P., Neil, H.L., Pospelova, V., Qi, Y., Radi, T., Richerol, T., Rochon, A., Sangiorgi, F., Solignac, S., Turon, J.-L., Verleye, T., Wang, Y., Wang, Z., Young, M., 2013. Atlas of modern dinoflagellate cyst distribution based on 2405 data points. *Rev. Palaeobot. Palynol.* 191, 1–197.

Zumaque, J., Eynaud, F., Zaragosi, S., Marret, F., Matsuzaki, K.M., Kissel, C., Roche, D.M., Malaizé, B., Michel, E., Billy, I., Richter, T., Palis, E., 2012. An

Ocean–ice coupled response during the last glacial: zooming on the marine isotopic stage 3 south of the Faeroe Shetland Gateway. *Clim. Past* 8, 1997–2017.

Zweng, M.M., Reagan, J.R., Antonov, J.I., Locarnini, R.A., Mishonov, A.V., Boyer, T.P., Garcia, H.E., Baranova, O.K., Johnson, D.R., Seidov, D., Biddle, M. M., 2013. World Ocean Atlas 2013, Volume 2: Salinity. In: Levitus, S., Mishonov, A. (Eds.), NOAA Atlas, 74, NESDIS, pp. 39.